Short term control of the cardiovascular system: Assessment with the isometric handgrip exercise

Claire Médigue, Yves Papelier, Sylvain Bise, Michel Sorine

INRIA

INSTITUT NATIONAL DE RECHERCHE EN INFORMATIQUE ET EN AUTOMATIQUE

Short term control of the cardiovascular system: Assessment with the isometric handgrip exercise.

Claire Médigue — Yves Papelier — Sylvain Bise — Michel Sorine

N° 5234

June 18, 2004

THÈME 1

ISSN 0249-6399 ISRN INRIA/RR--5234--FR+ENG

Short term control of the cardiovascular system: Assessment with the isometric handgrip exercise.

Claire Médigue , Yves Papelier , Sylvain Bise , Michel Sorine

Thème 1 —Réseaux et systèmes
Projet SOSSO2

Rapport de recherche n° 5234 —June 18, 2004 — 46 pages

Abstract: This study aims at assessing the short term control of the Cardio Vascular system (CV), through a physiological test which involves strictly autonomic response: the handgrip isometric exercise, under vagal influence during the first minute. CVS parameters are extracted from RR and the arterial blood pressure (ABP) signals, respectively giving frequency and amplitude information on the CVS. Mean time series, spectral values and baroreflex sensitivity (BRS), seen as the spectral controller gain between RR and ABP, help to approach the underlying mechanisms of the autonomic control. Results give evidence of two major effects:
- The relation between heart rate and contractility (positive staircase or Treppe effect).
- The drop of BRS, due to the decrease of heart variability.

Key-words: Autonomic Nervous System, Cardiovascular System, Cardiovascular Variability, Baroreflex Sensitivity, Treppe effect, positive staircase

Unité de recherche INRIA Rocquencourt

Contrôle à court terme du système cardiovasculaire: Evaluation avec l'exercice isométrique du handgrip

Résumé : Cette étude s'intéresse au contrôle à court terme du Système CardioVasculaire (SCV) à travers un test physiologique qui déclenche des réponses strictement autonomiques: l' exercice isométrique ou "Handgrip test", sous influence parasympathique pendant la première minute. Des paramètres du SCV sont extraits des signaux RR et de pression artérielle, donnant respectivement les informations en fréquence et en amplitude du SCV. Les valeurs temporelles moyennes, spectrales et la sensibilité baroréflexe, vue comme le gain spectral entre RR et ABP, aident à comprendre les mécanismes sous-jacents du contrôle autonomique. Les resultats mettent en évidence deux effets majeurs:
- La relation entre fréquence cardiaque et contractilité (escalier positif ou effet Treppe).
- La chute de la sensibilité baroréflexe, due à la diminution de la variabilité cardiaque.

Mots-clés : Système Nerveux Autonome, Système Cardiovasculaire, Variabilité Cardiovasculaire, Sensibilité Baroréflexe, relation fréquence-force, effet Treppe,escalier positif

Contents

1 Background

1.1 Short term control of the cardiovascular system (CVS) by the autonomic nervous system (ANS) at rest

The ANS regulates blood flow with respect of pressure constraints. This regulation at rest is seen as a closed loop, where the ANS is the controller, the baroreceptor the sensor and the heart the actuator and is usually called the baroreflex [36].

The intrinsic cardiac depolarisation is propagated through the conduction network: from the atrial sinus node (i.e, the cardiac pace-maker), to the atrio-ventricular node, the His bundle and the Purkinje fibers (Fig.1). Contractile cells do not initiate their own action potential, but the excitation is propagated by gap junctions which allow rapid conduction and coordinated contraction (Fig.2).

The two components of the ANS have antagonist direct actions on the heart; the sympathetic tone increases heart rate (chronotropic effect on the sinus node), conduction (dromotropic effect on the atrio-ventricular node) and contractility (inotropic effect on the myocardial cells), while the parasympathetic (or vagal) has only chronotropic and dromotropic direct negative effects (Fig.3). Sympathetic and parasympathetic effects on heart function are mediated by beta-adrenoceptors and muscarinic receptors, respectively. The vagal fibers have afferences to the sinus node and the atrio-ventricular node, thus only at the atrial level. The sympathetic fibers have afferences on all the myocardiac cells [25], [22], [3]. They act through the sinus node on the conduction network but also on the myocardial cells in the atrium and the ventricle.

At rest, the heart is continuously modulated by these two autonomic components and the parasympathetic inhibition is larger than the sympathetic stimulation (Fig.5). The intrinsic spontaneous heart rate is around 100-110 bpm. The parasympathetic influence slowers the resting heart rate down to 60-80 bpm while the sympathetic influence increases it to 200 bpm during heavy exercise (Fig.6). There is reciprocal inhibition between the two ANS components (Fig.4).

Vessels are under sympathetic influence, which increases peripheral vasoconstriction.

1.1.1 Chronotropic action of the ANS on the sinus node: heart rate modification

In autorhythmic cells, the pacemaker potential is unstable and determined by ionic currents: Na^+ inward, K^+ outward, Ca^{2+} inward (Fig.7,8). The ANS modifies the ionic currents. The parasympathetic nerve stimulation: a- increases the K^+ conductance (increased K^+ efflux), resulting in hyperpolarisation of cells, lowering the DMP; b- decreases the Ca^{2+} current (decreased Ca^{2+} influx), slowing the depolarisation rate of the PP, leading to bradycardia (Fig.9,10). The sympathetic nerve stimulation increases slow Ca^{2+} inward and Na^+ inward, increasing the slope of PP; at the same time the threshold potential, TP, is lowered leading to tachycardia (Fig.10).

1.1.2 Inotropic action of the ANS on the myocardial cells: heart contractility modification

Increase in contractility is due to increase in cytosolic Ca^{2+}. A direct inotropic action is produced by adrenergic $beta_1$ receptors. Meanwhile, an indirect inotropic action can be induced by an increase in heart rate (Fig.3). Cardiac acceleration reduces the diastole duration and thus decreases the Ca^{2+} outward, leading to a higher Ca^{2+} concentration in the cytosol. Cardiac deceleration has the opposite effect, leading to a decrease in intracellular Ca^{2+}, thus in contractility. Mechanisms underlying this action, so called “treppe” or “positive staircase” effect, are under investigation at molecular levels in human normal and failing myocardial cells [1, 61] and in mouse [2, 21, 17]. Mohrman and Heller (page 45-46) and Katz (pages 323-324, Physiology of the Heart, 2nd ed., by Arnold M. Katz, Raven Press, 1992.) also discuss the underlying mechanisms that account for this intrinsic regulatory phenomenon.

Other references: http://www.cvphysiology.com/ (Richard E. Klabunde); http://www.sfu.ca/, Lecture Notes from

Silverthorn, D.U. (2003) Human Physiology: An integrated approach, 3rd Edition; Atlas de poche de physiologie, S. Silbernagl, A. Despopoulos, Flammarion, 3rd Edition; Comprendre la physiologie cardiovasculaire, E.P D'Alché, Flammarion, 2nd Edition.

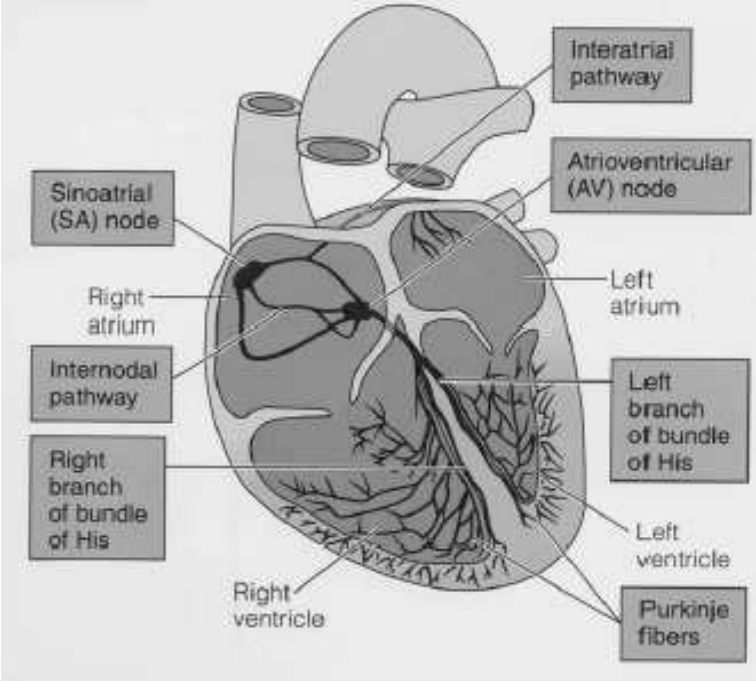

Figure 1: *Intrinsic Conduction System of the heart*

1.2 The handgrip test

Isometric exercise is well suited to investigate short term control of the cardiovascular system by the ANS: at any rate of maximum voluntary contractions (MVC) the static handgrip alters the baroreflex functionning, bringing about marked increases in heart rate and arterial pressure. The cardiovascular response within the first minute is driven to the heart through a rapid parasympathetic withdrawal, without consistent sympathetic activation. On the contrary, a vasodilatation occurs in the nonexercising forearm at the beginning of isometric exercise, due to cholinergic mechanisms, showing a dissociation between sympathetic nerve activity and forearm vascular responses [53]. The sympathetic activation then depends on the duration and intensity of the exercise: mild to moderate-intensity exercises (for Hansen, from 20 to 33% MVC) do not evoke sympathetic activation contrary to high-intensity exercises (for Hansen 45% MVC) [14], [56], [58], [57], [65], [23], [62], [64], [52].

1.2.1 Alteration of the short term controller mechanisms

This cardiovascular response is thought to be mediated by two fast mechanisms (Fig.11):

First, the voluntary central command, arising at the onset of any kind of exercise, leads to a synchronous activation of the motor and cardiovascular systems [**?**], [15], [29], [38]. This activation results in an indirect but very fast stimulation of cardiovascular centers by descending collateral signals [**?**], [16], [15], [29], [66], as

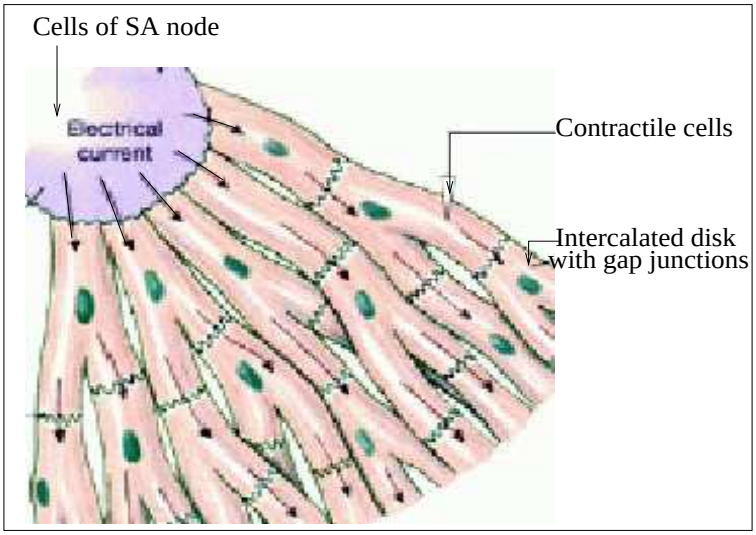

Figure 2: *Autorhythmic and contractile cardiac cells*

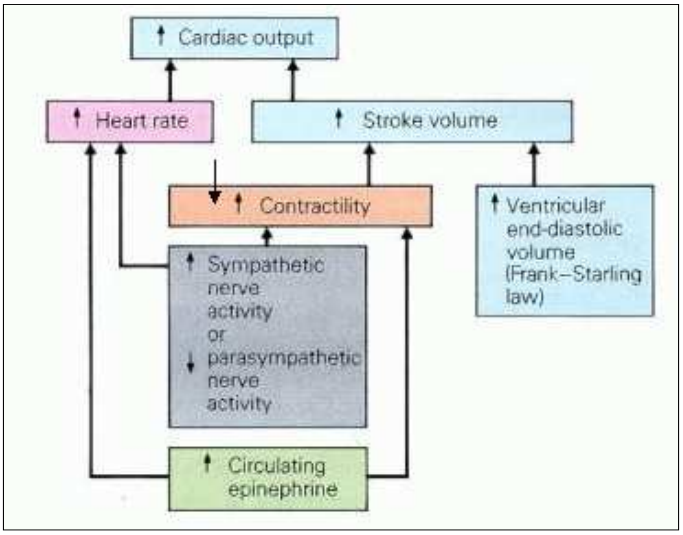

Figure 3: *Global heart control: mechanical, autonomic and hormonal. Autonomic control influences heart rate and contractility. Heart rate influences contractility.*

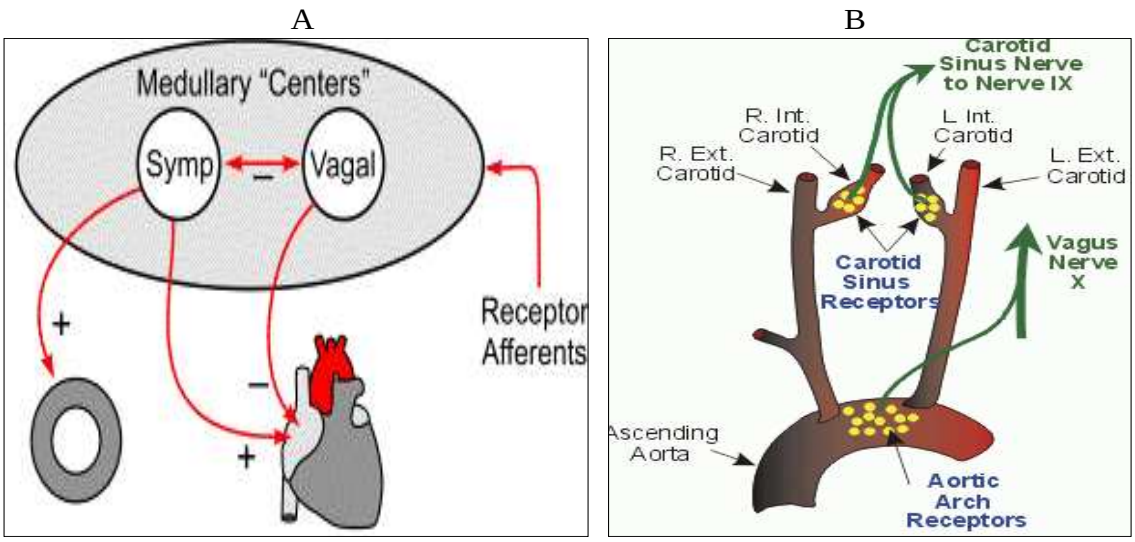

Figure 4: *A: reciprocal inhibition between sympathetic and vagal medullary centers. B: baroreceptors location and innervation.*

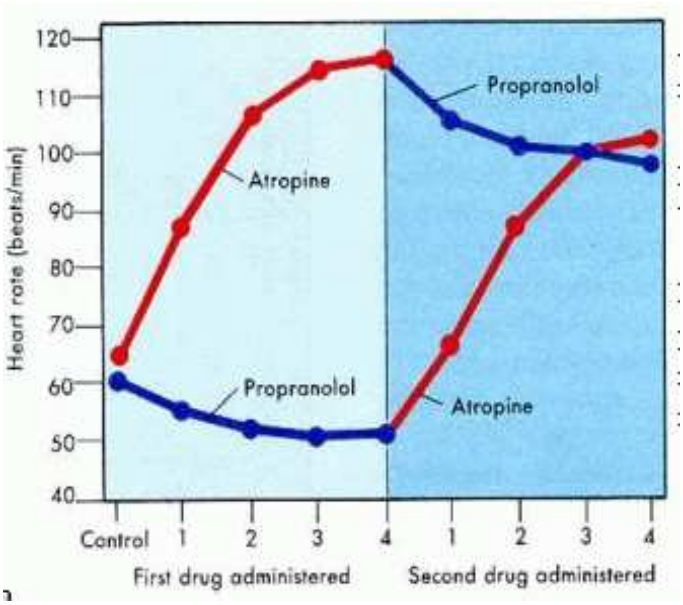

Figure 5: *Resting autonomic control of heart rate. Atropine is a parasympathetic antagonist, propanolol a sympathetic antagonist.*

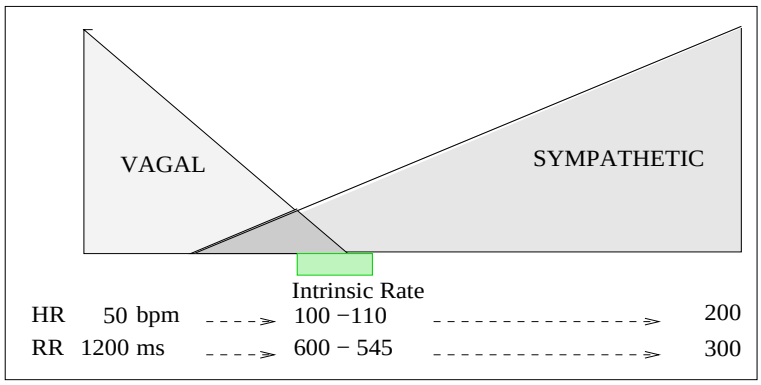

Figure 6: *Heart rate: intrinsic rate and autonomic influence*

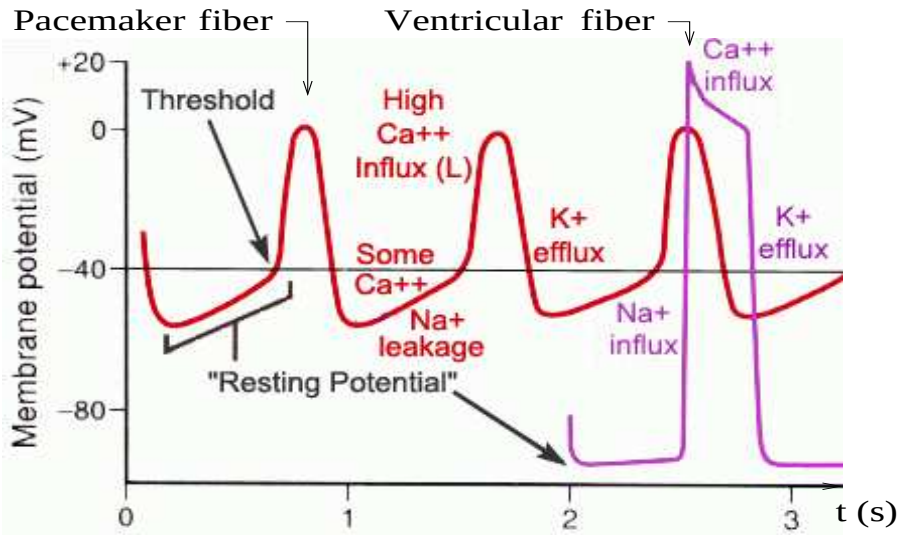

Figure 7: *Superposed pacemaker and ventricular fibers ionic currents. ANS influences the unstable resting potential of the pacemaker fiber and the action potential of the ventricular fiber.*

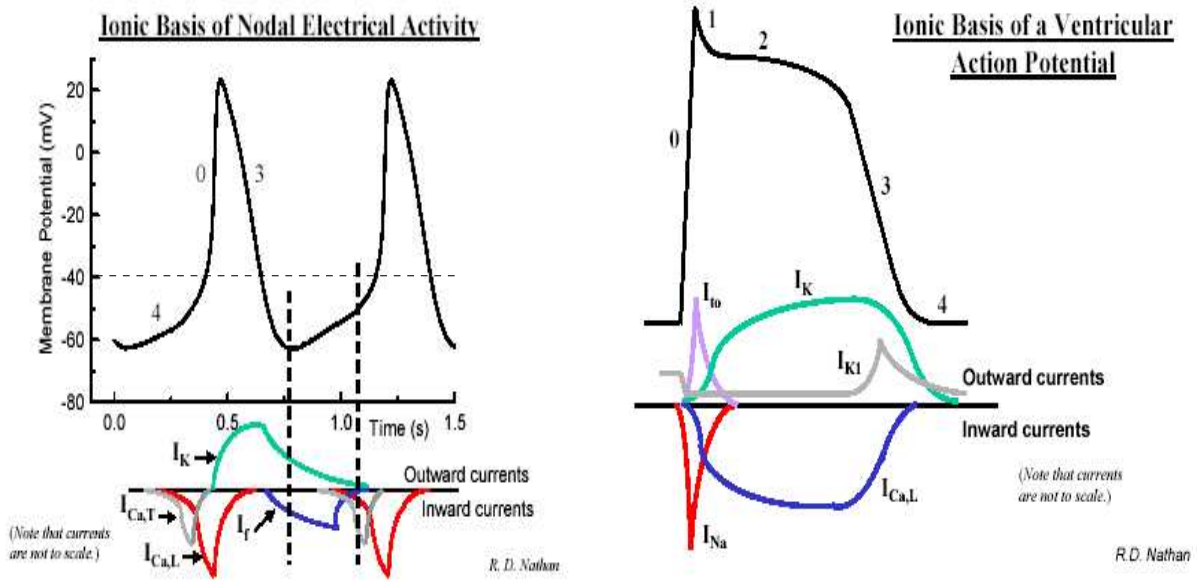

Figure 8: *Details of ionic durrents for the two cells.*

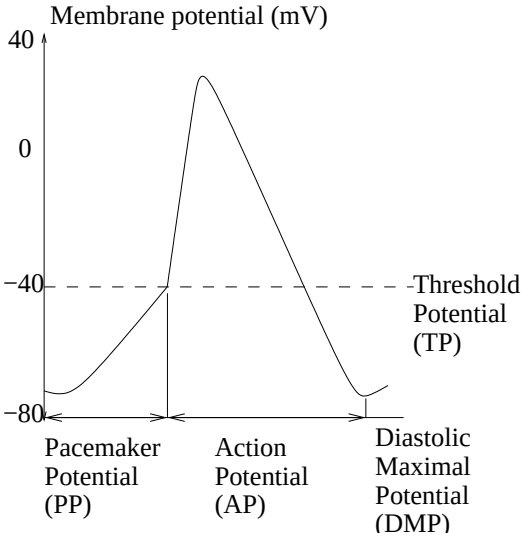

Figure 9: *Pacemaker activity*

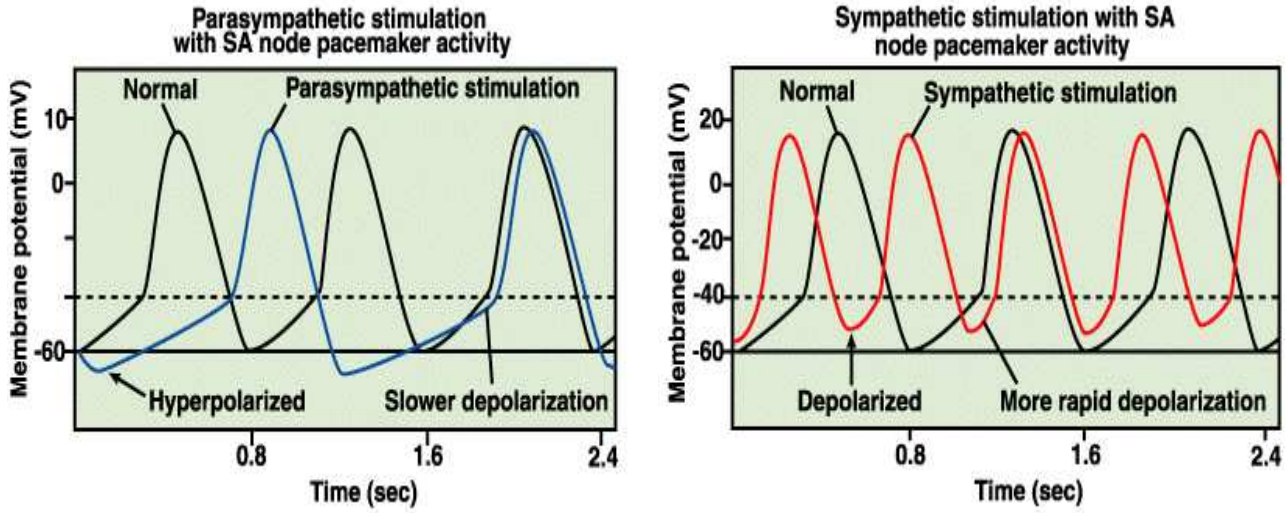

Figure 10: *Autonomic influence on the resting pacemaker potential (PP).*

though the system anticipated the hypothetical oxygen muscle needs. Therefore this mechanism can be considered as a feedforward.

Second, a peripheral stimulation of ergoreceptors (mechanoreceptors) [31], [47] sensitive to muscle stretching, via the afferent nerves (group III and IV fibres) originating in the working muscle group, could participate to the cardiovascular response via arterial and cardiopulmonary baroreflexes [51]. Therefore this mechanism can be considered as a feedback.

1.2.2 Sensor modification involved in the handgrip test

As a result in those two cases, the operating point of the baroreflex response curve rapidly offsets to higher values of aortic and carotid sinus pressures [44], [49]. So, the prevailing blood pressure is “read” as lower than the new operating point due to the offset, and before any change in needs for oxygen, the arterial baroreflex triggers increases in heart rate, blood pressure and thus in cardiac output (Fig.12,13). .

Our aim is to better understand the autonomic behavior during a one minute handgrip test, through cardiovascular parameters alterations. Indeed, the first minute of an handgrip test is an exceptional physiological condition of pure parasympathetic response, resulting in cardiac acceleration, blood pressure augmentation and alteration of cardiovascular parameters variabilities. Very few studies have utilised heart rate variability (HRV) during handgrip exercise [23], [24]. This study analyses not only heart rate variability but also blood pressure variability. The spectral gain between heart rate and arterial blood pressure, considered as input and output of the baroreflex loop, could provide a useful insight in neural autonomic control of the cardiovascular system.

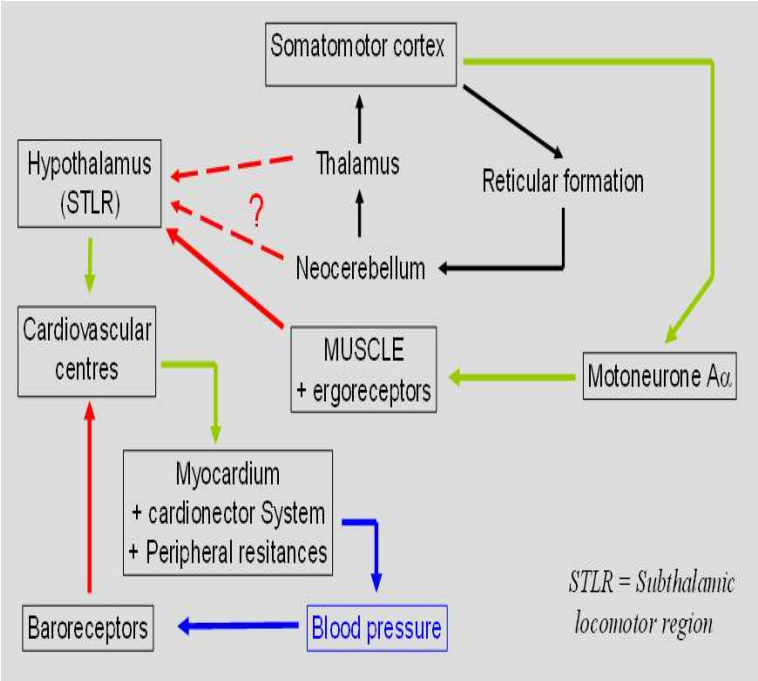

Figure 11: *Cardiovascular centers implied in the baroreflex offsetting*

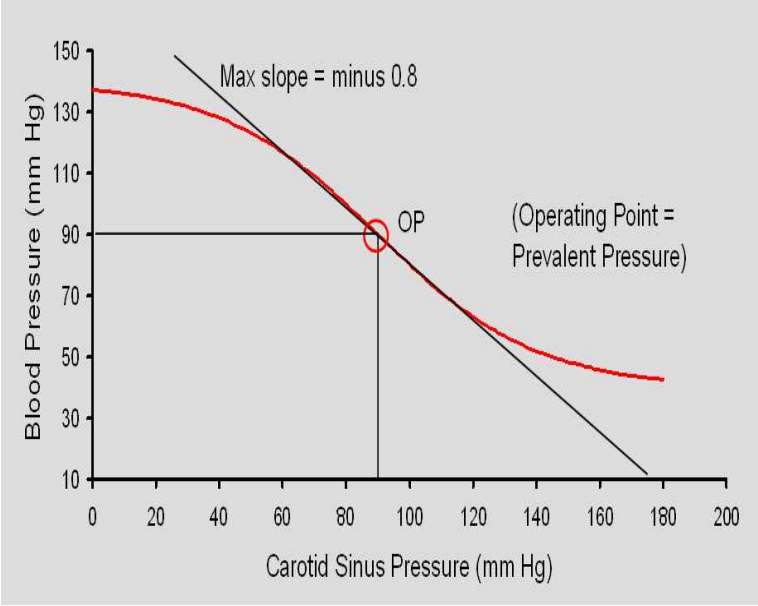

Figure 12: *Baroreflex response curve at rest*

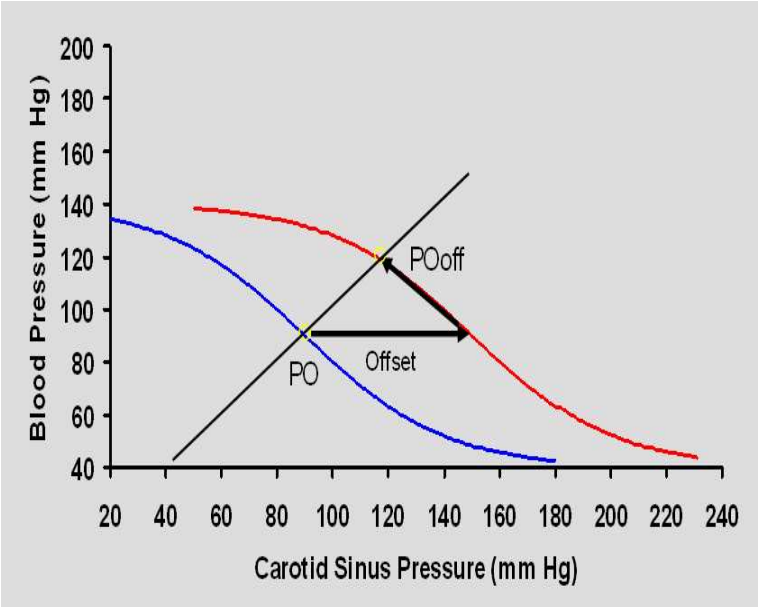

Figure 13: *Offset of the baroreflex response curve during the handgrip test*

2 Meaning of cardiovascular parameters

2.1 Cardiovascular variability

RR variability reflects beat-to-beat modulation by sympathetic and parasympathetic cardiac afferents. RR high-frequency (HF_{RR}) reflects mostly vagal modulation ([26], [27], [40]) and relates to respiratory oscillations whereas RR low-frequency (LF_{RR}) seems to depend upon both sympathetic and parasympathetic modulations ([10], [18], [26], [45]).
The blood pressure low-frequency component (LF_{ABP}) is considered as a marker of vascular sympathetic modulation ([40], [9]) whereas the HF blood pressure component (HF_{ABP}) reflects the mechanical influence of the respiration on the CV system ([45]).

2.2 Mean heart rate and heart rate variability

They provide different informations on the autonomic nervous system (ANS) behavior. Various experiments, described in [36] suggest that they could be controlled by two different mechanisms ([35], [30], [28], [13]). RR variability could represent the sympathovagal modulation to the sinus node activity whereas mean RR could represent the tonic neural control, a global measure of the sympatho-vagal tone. To have an overview of the sympathovagal balance, RR-interval can be estimated by normalised spectral values, such as $HFnu_{RR}$, $LFnu_{RR}$ or HF_{RR}/LF_{RR}. So, normalised units represent the concept of a balance beam pivoted around its center, that corresponds to mean RR value. Nowadays, non invasive estimation of cardiac nerves activity is mainly based upon results obtained from RR relative spectral power. The meaning of spectral absolute values is still now poorly understood and therefore very often neglected.
In this study, we propose an hypothesis which takes into account the differences between mean RR and RR variability behavior, and which could explain the spectral absolute values behavior.

2.3 Baroreflex sensitivity (BRS)

BRS can be seen as the controller gain between ABP and RR, considering the ABP as one of the inputs and the RR as one of the outputs of the baroreflex system, with a linear input-output relationship. The figure 14 shows the two transfer functions H_{hemo} and H_{contr}: H_{hemo} is the hemodynamic transfer from (RR,n_{RR},R_{centr}) and ABP and H_{contr} is the neural feedback transfer from (ABP,n_{ABP},R_{mech}) and RR. The baroreflex sensitivity is represented by H_{contr}.
The respiratory activity can have a central effect, directly leading to respiratory sinusal arrythmia (RSA) and through H_{hemo}, to ABP oscillations; and a mechanical effect, directly leading to ABP oscillations, and through H_{contr}, to RSA. BRS, defined as the controller gain between SBP and RR, presumes a permanent and linear association between them. A minimal central direct influence of respiration is supposed, so that RR is related to SBP in a linear way ([39]).
BRS is a frequency-band dependent phenomenon revealing different autonomic mechanisms ([28], [46], [48]). The long term BRS (gLF_{SBP}, gLF_{DBP}) acts on slow CV oscillations (Mayer waves, around 10 s), whereas the short term BRS (gHF_{SBP}, gHF_{DBP}) acts on fast CV oscillations, related to breathing oscillations. Both measurements together give a better insight on the cardiovascular autonomic control (18). In day-time studies, BRS has been assessed in both the LF band ([19], [39], [42], [50], [9]) and HF band ([28], [39], [48]).

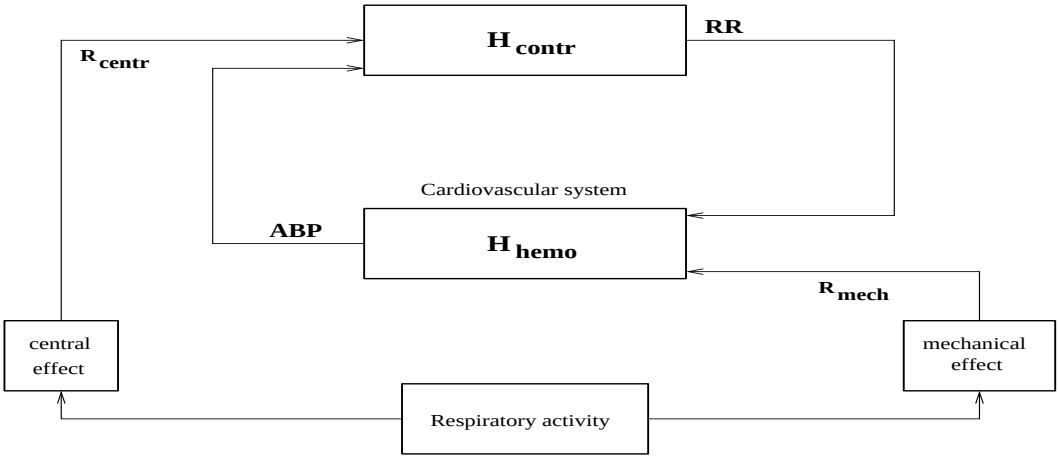

Figure 14: *Simplified diagram of closed-loop neural reflex with only the control of the ABP made by RR-interval. H_{hemo} is the hemodynamic transfer from (RR,n_{RR},R_{centr}) and ABP and H_{contr} is the neural feedback transfer from (ABP,n_{ABP},R_{mech}) and RR.*

3 Physiological methodology: subjects, protocol and data acquisition

3.1 Subjects

Height healthy male subjects gave a written informed consent to participate in this study. The subjects were non-smokers and none was taking any medication. The experimental protocol and consent form were approved by the university review board for health sciences research involving human subjects.

3.2 Physiological protocol

Each of the subjects exercised at the same time of the day. Prior to the experiment the subject was instructed to avoid strenuous exercise within the day preceding the test date, to have only a light meal, and to restrain from beverages containing caffeine for 12h preceding the test. After entering the test room, each subject sat on a comfortable armchair. The handgrip dynamometer was constituted of a calibrated strain gauge fitted to an anatomic handle. As a warm-up the subject performed a ramp of 5 seconds graded voluntary contractions, broken by one-minute recovery phases between two contractions. The subject can assess his strength by a visual feedback (biofeedback) through an oscilloscope display (PowerLab, ADInstruments, Australia). Step increase was 10 daN, with a 30 second recovery between two steps, until maximum voluntary contraction (MVC) was reached. The warm-up enables us to determine the precise level corresponding to 40 % MVC. After an interval of about 5 min, the subject performed the test constituted of five successive 60 seconds phases of isometric handgrip exercise at 40% MVC, broken with 2 minute bouts of recovery between two handgrip phases.

3.3 Data acquisition

During warm-up and test, ECG, continuous blood pressure, ventilatory outflow and strength were monitored and recorded at a 1000 Hz-sampling, using an A/D apparatus (PowerLab, ADInstruments, Australia).

4 Signal processing methodology

The data were processed in LARY-C, a software package dedicated to the study of cardiovascular and respiratory rhythms, developed in the SCILAB_SCICOS environment [37]. The theorical aspects of the implemented methods refers to the INRIA Research Report "Short-term control of the cardiovascular system: modelling and signal analysis" n^o4427 (http://www.inria.fr/rrrt/rr-4427.html) [36].

4.1 Preprocessing: events detection, resampling and filtering

For building the RR time series, an adaptive threshold algorithm was applied to the derivative of the ECG. SBP was determined by a modified version of Pan's algorithm [41] and DBP was the first minimal diastolic point detected preceeding the SBP value, on the raw arterial blood pressure. The resulting signals, RR time series, SBP and DBP time series and the raw Force signal were then resampled at 4 Hz, by spline interpolation. Then, for improving FFT results, we applied a Finite Impulsionnel Response filter (FIR filter) before FFT calculation, to keep only frequency bands of interest, fixed in [0.03 - 0.5] Hz; the corresponding SCICOS block is *WFIR* on the figure 15.

4.2 Spectral Evaluations and Baroreflex Sensitivity

4.2.1 Spectral Evaluations

A 128-point FFT, overlapped by half, was applied to CV data segments, to obtain CV parameters on 32 seconds bouts. A smoothing of the power spectral density (SPSD) with a 5-points rectangular moving average was applied to reduce spectral variance and to provide the Smoothed Power Spectral Density for each RR, SBP/DBP spectrum (block *smooth* on fig.15).

4.2.2 Baroreflex Sensitivity

As described in the background, BRS assumes a linear association between RR and ABP. So, we first performed a Cross Spectral Analysis between RR and SBP/DBP to assess the Coherence Function between SBP/DBP and

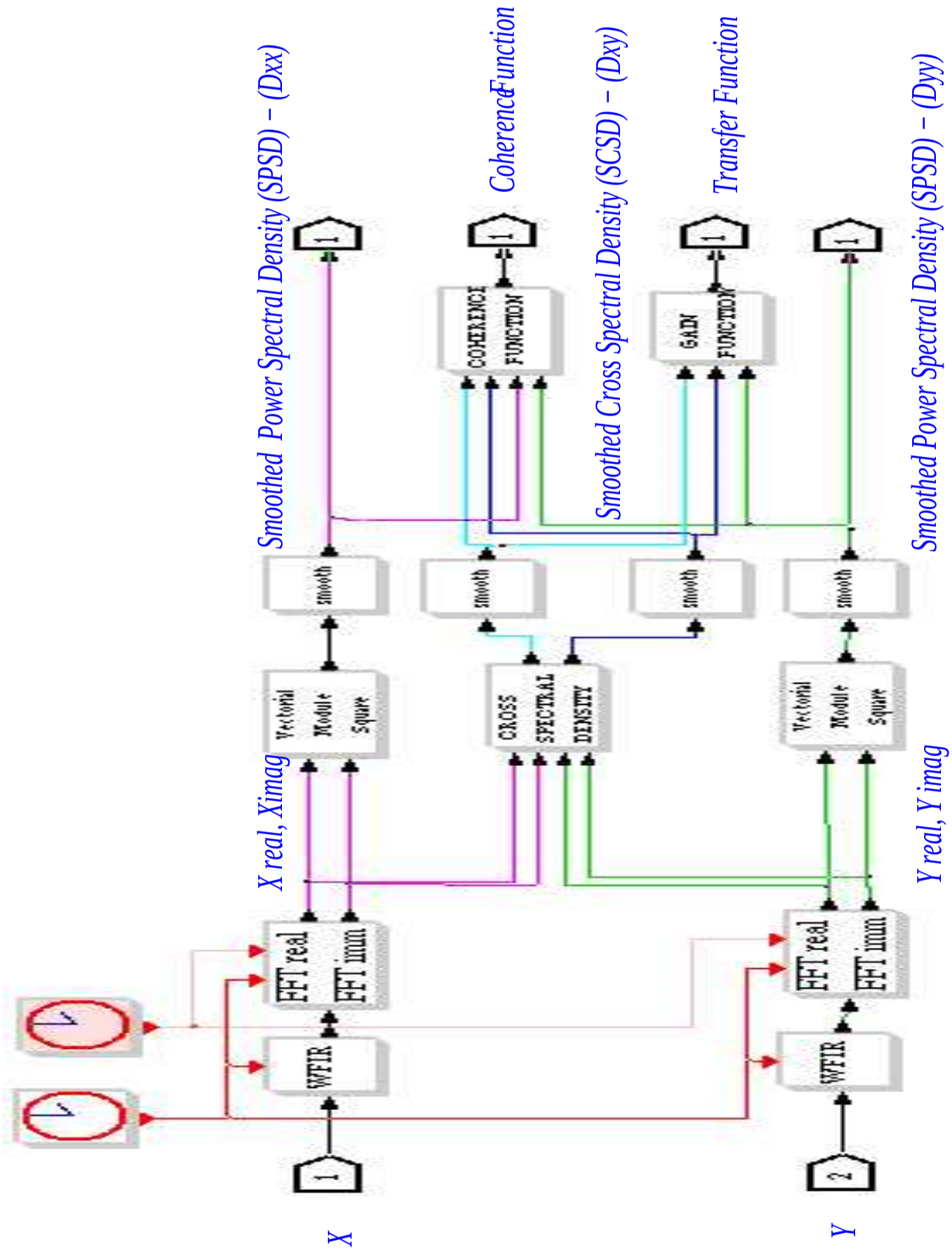

Figure 15: *Flow chart of the Gain assessment: SCICOS blocks*

RR. Coherence function in (0;1), provides an estimation of the degree of linearity between two signals. Only epochs with coherence values greater than 0.5, validating the hypothesis of linearity, allowed the computation of the averaged gain (blocks *Cross Spectral Density, Coherence Function, Gain Function* on fig.15). The figure 16 gives an example of the Coherence and Gain between two synthetic signals, selected in the [0.05 - 0.15]Hz frequency band.

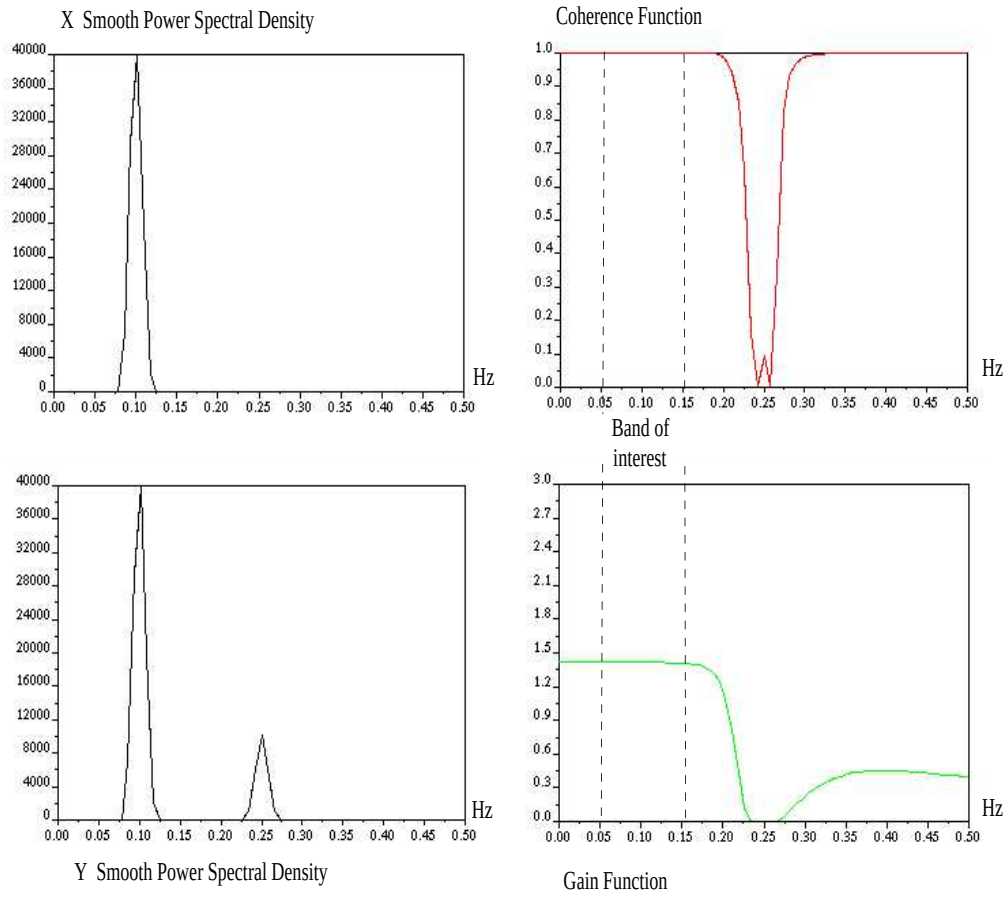

Figure 16: *Spectral features of the SPSD, Coherence and gain*

4.2.3 Spectral evaluation and Baroreflex Sensitivity in HF and LF bands

Spectral components, Coherence and Gain were then extracted in the two frequency bands of interest, HF and LF. Breathing frequency (BF) was estimated for each subject, looking at the high frequency component in their RR spectrum. For all the subjects, BF was contained between 0.15- 0.5 Hz, allowing us to define a global HF band as [0.15 - 0.5] Hz. The central frequency (CF) of the HF spectrum of the RR time series and it's dispersion around

CF were calculated. The dispersion index (DI) provides an estimation of the regularity of the breathing activity; DI takes values in (0;1). The more regular is the breathing activity, the smaller the DI is. LF band was fixed to [0.03 - 0.15Hz), according to the Task Force [11]. The power of the LF and HF components were computed as the area under SPSD in each band. RR spectral components were expressed in absolute values (LF_{RR}, HF_{RR}), in values normalised by the sum of LF_{RR} and HF_{RR} (LF_{RR}, HF_{RR}), as ms^2/Hz; LF_{BP}, HF_{BP} were expressed as $mmHg^2/Hz$. The gains gHF_{SBP}, gLF_{SBP},gHF_{DBP}, gLF_{DBP} were expressed as $ms/mmHg$.

4.2.4 Mathematical equations

Refer to the Research Report [36], [33], [35].

Spectral global evaluation

- *Complex Spectrum* $X(k\Delta f) = \sum_{i=0}^{N-1} x_i\, w_i\, e^{-j2\pi k\Delta f i T_o}$

  Where N=256 points, $T_o = 0.5\,s$ is the time-step of the resampled data series, w_i stands for i-th value of 256-Hanning window and $\Delta f = 1/T = 0.008Hz$ is the discrete frequency step (or spectral frequency resolution).

- *Smoothed Power Spectral Density* $\bar{D}_{xx}(k\Delta f) = \frac{1}{M+1} \sum_{l=k-\frac{M}{2}}^{k+\frac{M}{2}} D_{xx}(l\Delta f)$ in which M is odd (we fixed M=5).

- *Smoothed Cross Spectral Density* $\bar{D}_{xy}(k\Delta f) = \frac{1}{M+1} \sum_{l=k-\frac{M}{2}}^{k+\frac{M}{2}} X^*(l\Delta f)Y(l\Delta f)$

- Gain Function $|H_{xy}(k\Delta f)| = \frac{|\bar{D}_{xy}(k\Delta f)|}{\bar{D}_{xx}(k\Delta f)}$

- Coherence Function $\gamma^2_{xy}(k\Delta f) = \frac{|\bar{D}_{xy}(k\Delta f)|^2}{\bar{D}_{xx}(k\Delta f)\bar{D}_{yy}(k\Delta f)}$

Parameter evaluation in HF and LF bands

- **Energy:** $x_{FB} = \sum_{k\Delta f \in FB} \bar{D}_{xx}(k\Delta f)\ \frac{1}{\bar{x}}$
- **Gain:** $gain_{FB} = \frac{1}{\mathcal{L}_{FB}} \sum_{k\Delta f \in FB} |H_{xy}(k\Delta f)|\ \frac{\bar{x}}{\bar{y}}$
- **Coherence:** $coherence_{FB} = \frac{1}{\mathcal{L}_{FB}} \sum_{k\Delta f \in FB} \gamma^2_{xy}(k\Delta f)$

where the frequency band FB can be HF or LF, $\mathcal{L}_{FB}$ the bandwidth and $\bar{x}$ $\bar{y}$ the signal averages.

4.3 The Smooth Pseudo Wigner-Ville Distribution (SPWVD)

The SPWVD is a time frequency method, useful to follow the time "instantaneous" changes in spectral components of a signal. The SPWVD is defined as:

- $SPW_x^{N,M}(n,\omega) = \sum_{m=-\infty}^{+\infty} g_M(m) \sum_{k=-\infty}^{+\infty} h_N^2(k)\, x(n+k+m)\, x^*(n-k+m)\, e^{-j2\omega k}$

where N and M stand for the window sizes of h_N and g_M respectively. The window $g_M(m)$ determines the number of spectra involved in the average and hence the effectiveness for cross term suppression. The window $h_N(k)$ determines frequency smoothing of the SPWVD. Therefore, the two windows $g_M(m)$ and $h_N(k)$ perform smoothing in the time and frequency directions, respectively ([36], [34]).
In this study, SPWVD was used to visually underline the results which were separately obtained by FFT on handgrip and recovery stationary bouts. Indeed, changes in amplitude and frequency of the HF and LF CV components are continuously followed over all handgrip and recovery bouts (see fig.21, 22, 23).

4.4 Statistical analysis

Non parametric paired Wilcoxon tests were choosen, as they do not require the normality of the distribution, nor the equality of the variances. Indeed, they are based on rank and no on mean tests. They are robust for little samples [6]. They were applied on the mean RR and ABP values, spectral components and gains. All results are expressed as means and standard-deviation.
The 32 seconds FFT epochs were selected as following: first, consecutive epochs were discarded to avoid redundancy (they were overlapped by half) and epochs with coherence lower than 0.5. Then, the correct epochs were averaged over the second, third and fourth handgrip bouts, and over the following recovery bouts. It seems that the 2, 3 and 4th bouts exhibit comparable CV effects. For the first handgrip bout, CV reactions were often smaller and for the fifth, the exhaustion is probable.

5 Results

5.1 Mean cardiovascular values

Mean RR values are significantly lower during handgrip than during recovery bout: 811 versus 1025 ms. Mean ABP values are significantly higher during handgrip than recovery bouts: 183 versus 148 mmHg for SBP, 99 versus 80 mmHg for DBP. See Table 1 and Figure 17. Figure 17 shows mean RR and ABP time series during five successive one minute handgrips separated by two minutes recovery bouts, in one subject. This subject exhibits particularly clear reactions of withdrawal/stimulation of the vagal control on the heart and consequently on the ABP.

On the RR time series the suppression of the vagal brake provokes a more progressive cardiac reaction (acceleration) at the beginning of the handgrip than its recovery (deceleration) at the end. There is a reactional enhancement of the vagal activity at the beginning of the following recovery bout. A zoom on two handgrip followed by two recovery bouts (Fig.18) shows an augmentation of the amplitude in breathing oscillations (P=4 seconds) in the first 40-50 seconds of the recovery bouts.

The changes in SBP time series are very close to changes in heart rate, in timing as well as in slopes: FC acceleration/SBP augmentation and FC decceleration/SBP diminution. On Figure 19 the RR time series was converted in heart rate (HR time series), RR and SBP time series were pass-band filtered between 0.001 and 0.03 Hz to better compare the global changes in the two signals. Morever, zooming on the instant of the vagal brake recovery, Figure 20 shows on the raw signals the very fast SBP response to the FC decceleration ($< 2s$, i.e < 3 heart beats).

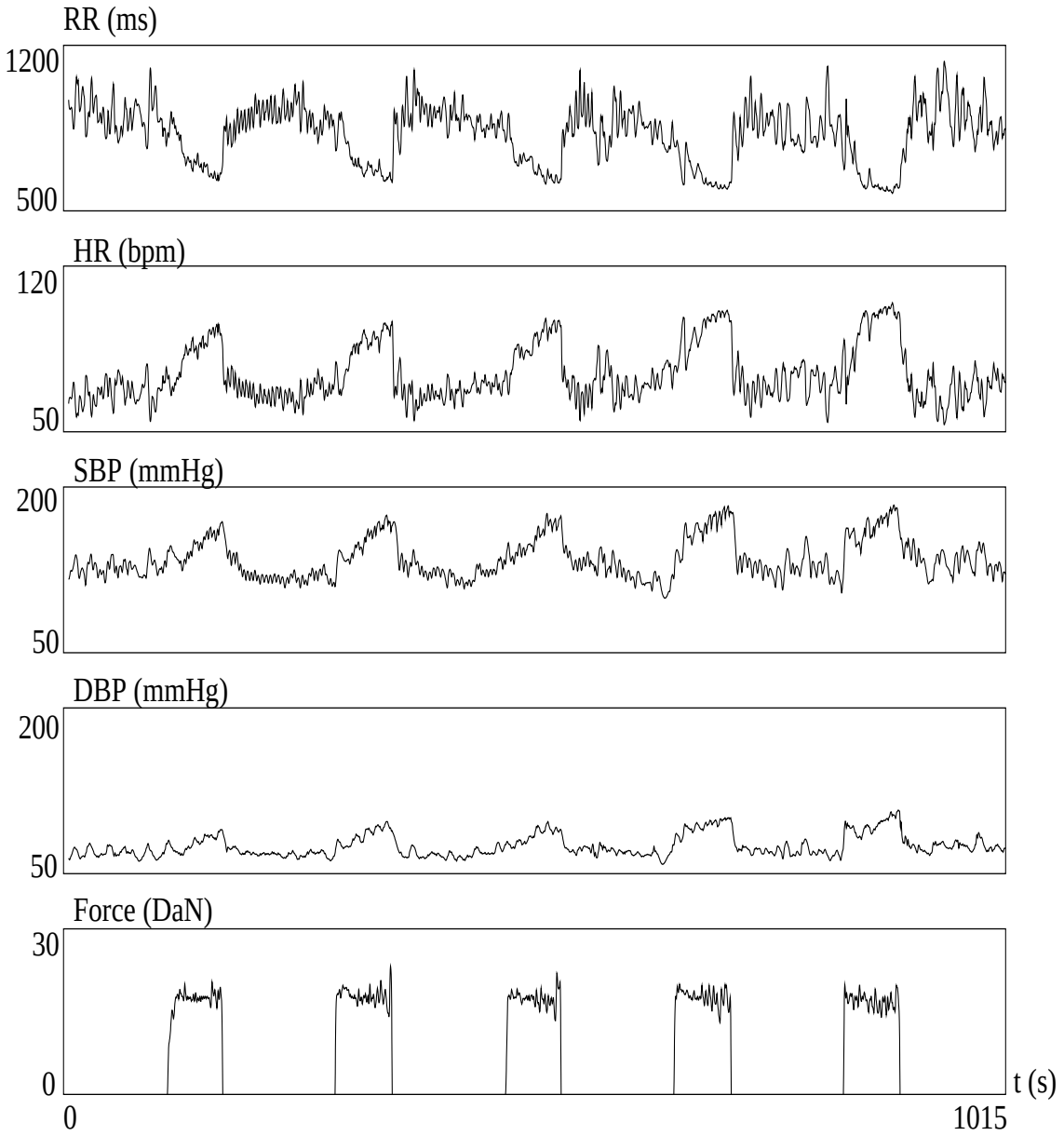

Figure 17: RR, HR, SBP, DBP time series during five handgrip bouts separated by recovery bouts, in one subject. Handgrip bouts are located by the force signal at the bottom. RR time series decreases, HR and the two ABP time series increase during handgrip bouts.

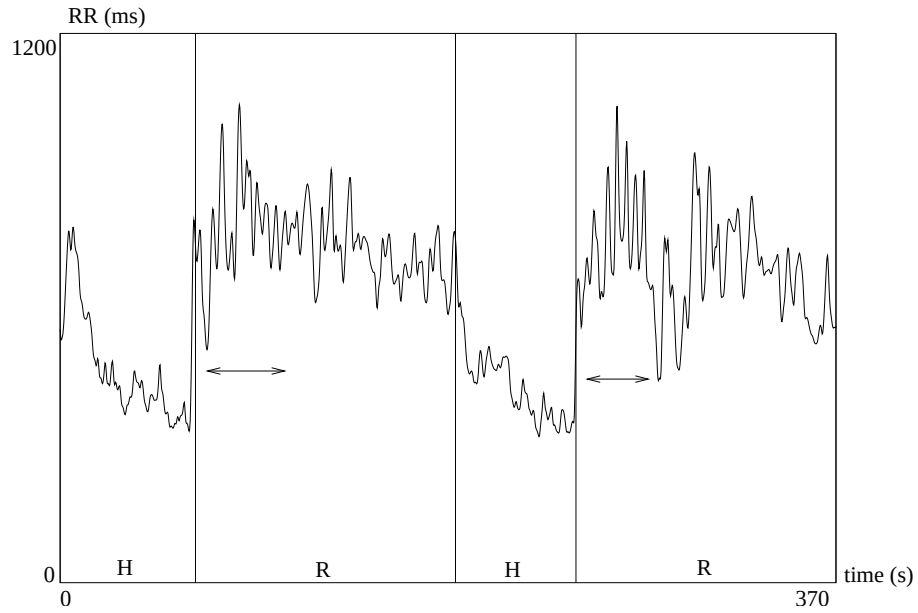

Figure 18: Zoom on the RR time series of one subject during two handgrip bouts (H) followed by two recovery bouts (R). The arrows underline the augmentation of the amplitude of breathing oscillations at the beginning of the recovery bout.

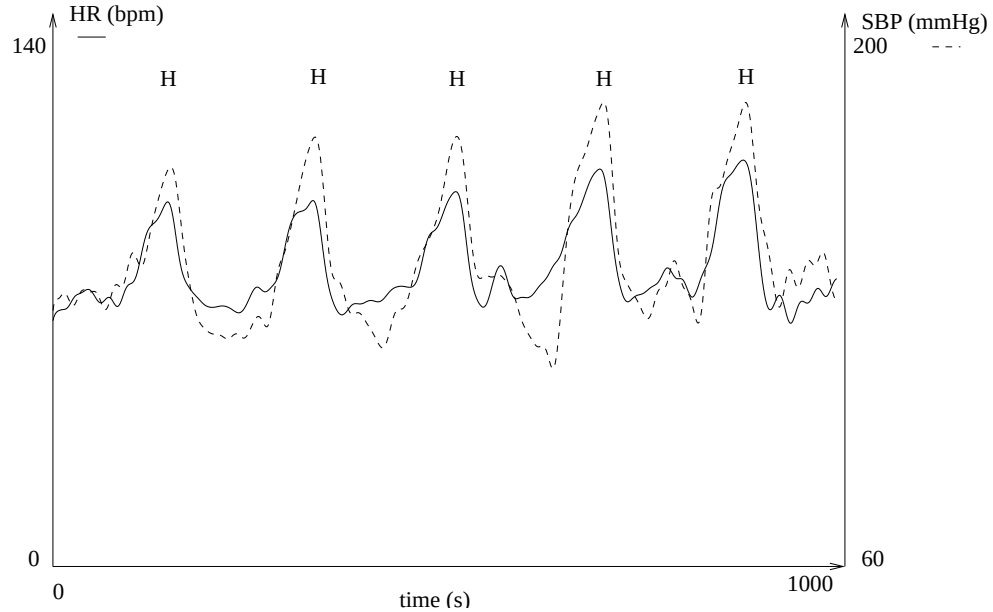

Figure 19: HR (continuous line) and SBP (dashed line) filtered time series of one subject during 5 handgrip bouts (H). The timing and the slopes of their changes are very close.

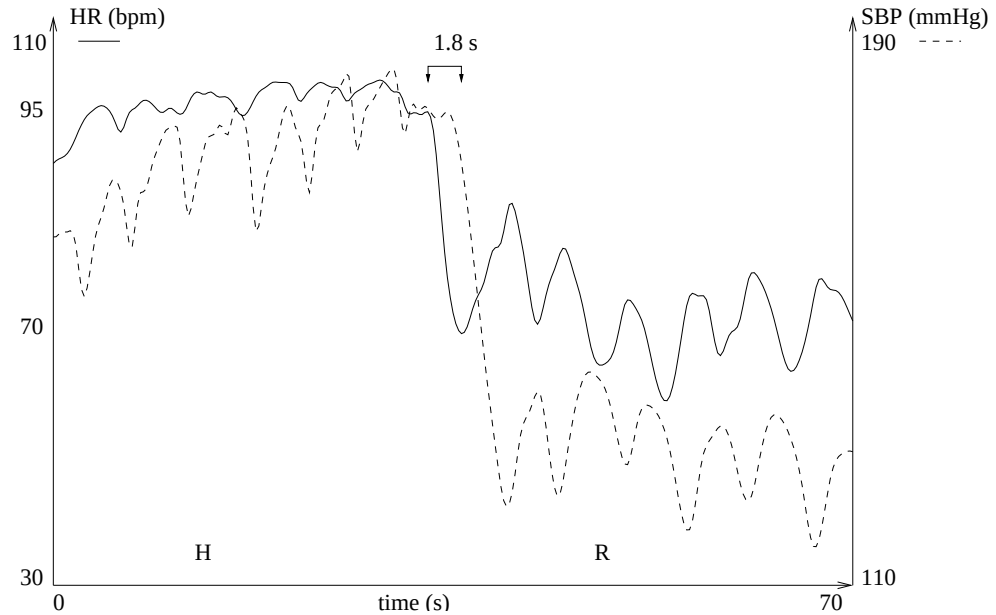

Figure 20: HR (continuous line) and SBP (dashed line) time series of one subject during the transition between an handgrip and a recovery bouts (H); The SBP response follows the HR by less than 2 seconds.

5.2 Cardiovascular variability

The power spectral values exhibit a strong difference between cardiac and arterial parameters changes in HF and LF bands during recovery versus handgrip bouts. The RR power spectral parameters (HF_{RR} and LF_{RR}) significantly fall together during handgrip bouts whereas the ABP power spectral parameters (HF_{SBP} LF_{SBP}, HF_{DBP} LF_{DBP}) do not significantly change (Table 1 and Fig.24). Figures 21 and 22 illustrate these results, showing the time evolution of the instantaneous amplitude of the HF and LF components of the CV signals, over three handgrip and four recovery bouts of one subject.
The central frequency (CF) of the HF spectrum and its dispersion (DI) in the RR and SBP time series exhibit no significant changes between recovery and handgrip bouts. Table 2 gives the mean values measured on epochs with coherence greater than 0.5 whereas Fig.23 shows the instantaneous frequency and amplitude in HF RR over all the protocole in one subject.

5.3 Baroreflex sensitivity

All gains significantly fall from recovery to handgrip bouts (Table3).

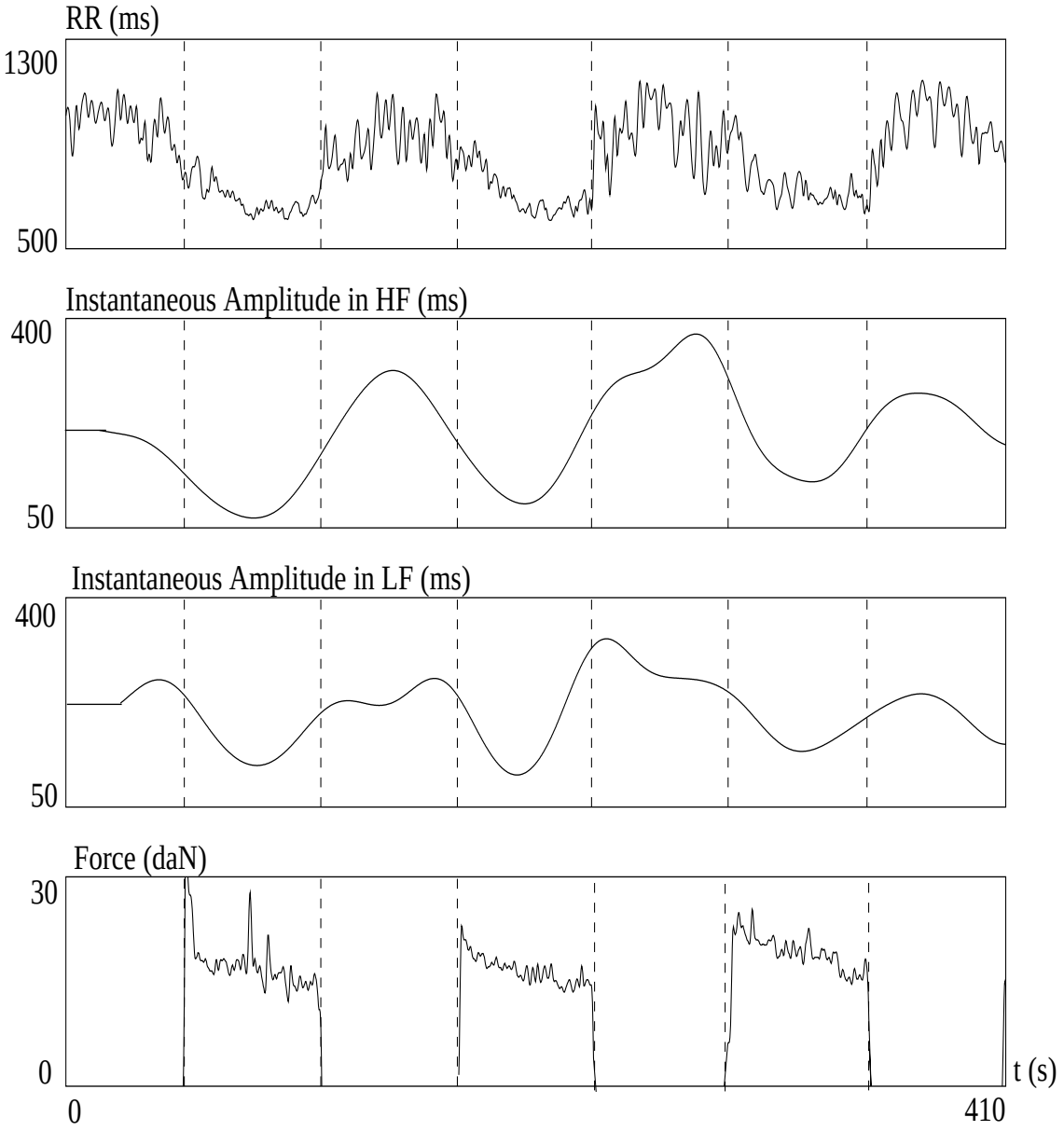

Figure 21: Instantaneous HF and LF spectral parameters for RR time series, during three handgrip bouts separated by recovery bouts, in one subject. Handgrip bouts are located by the force signal at the bottom. HF and LF amplitude fall during handgrip bouts.

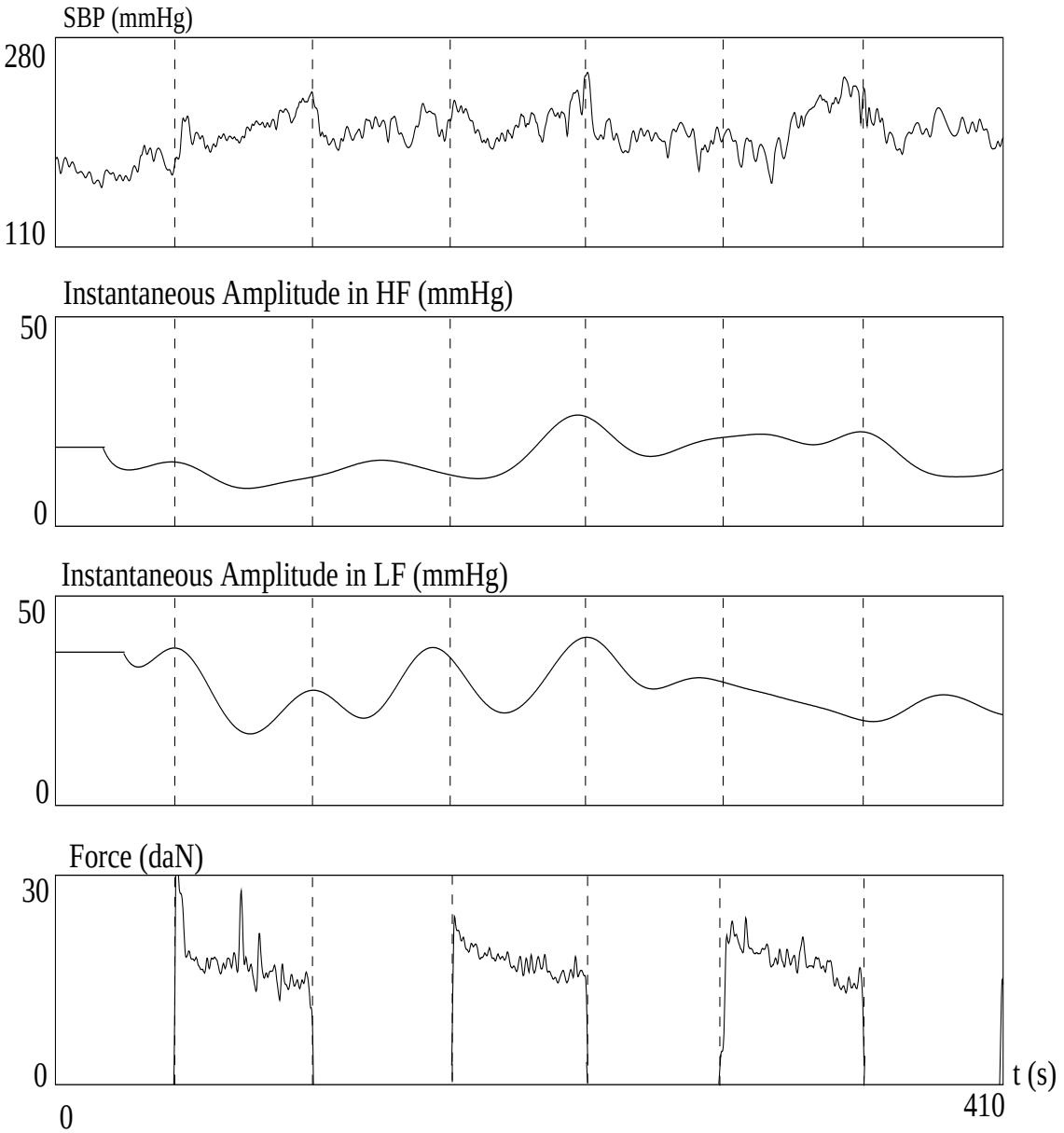

Figure 22: Instantaneous HF and LF spectral parameters for SBP time series during three handgrip bouts separated by recovery bouts, in one subject. Handgrip bouts are located by the force signal at the bottom. HF and LF amplitude have no significant change between recovery and handgrip bouts.

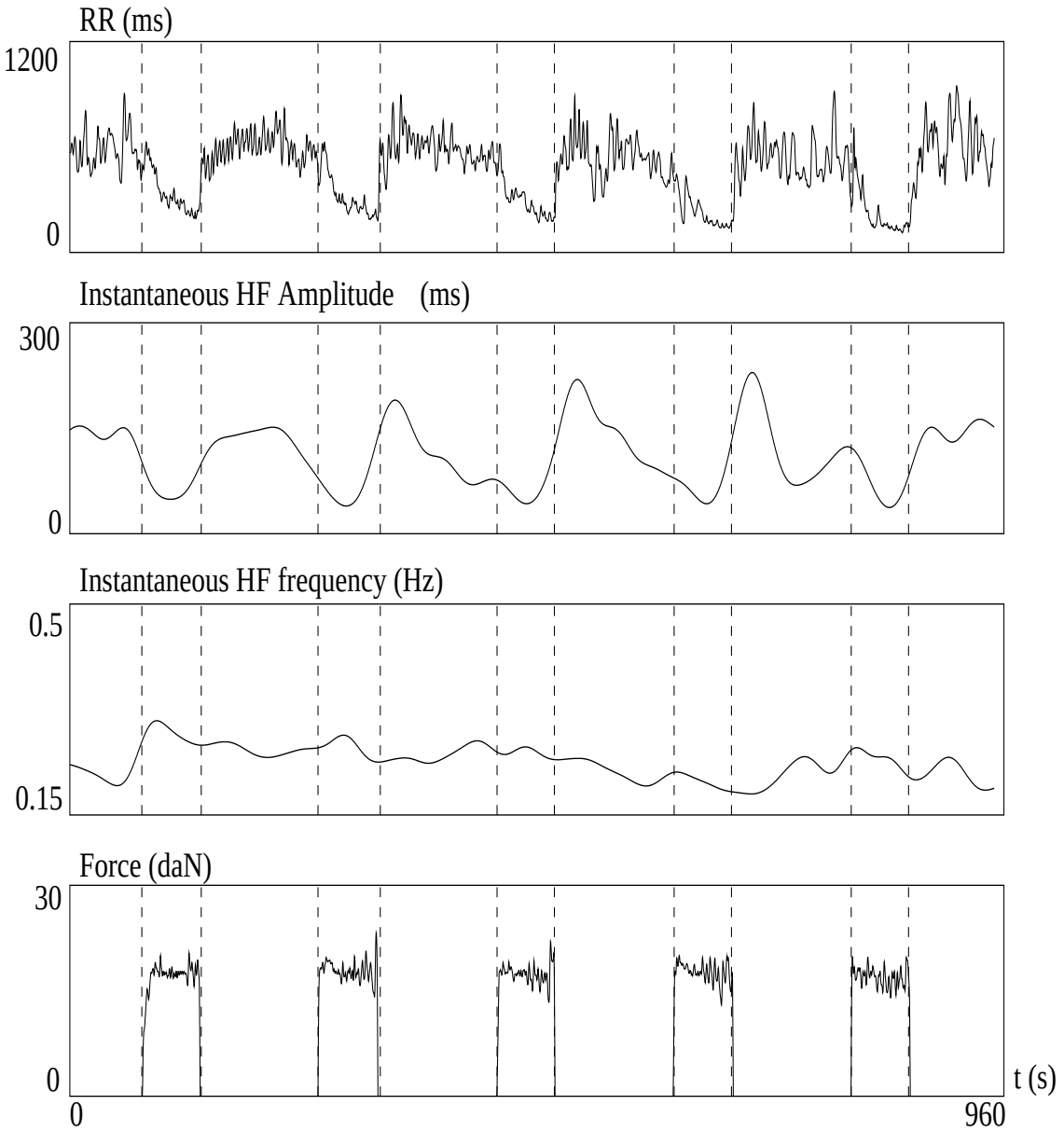

Figure 23: Instantaneous HF frequency and amplitude for RR time series during five handgrip bouts separated by recovery bouts, in one subject. Handgrip bouts are located by the force signal at the bottom. HF amplitude falls during handgrip bouts whereas HF frequency does not show significant change.

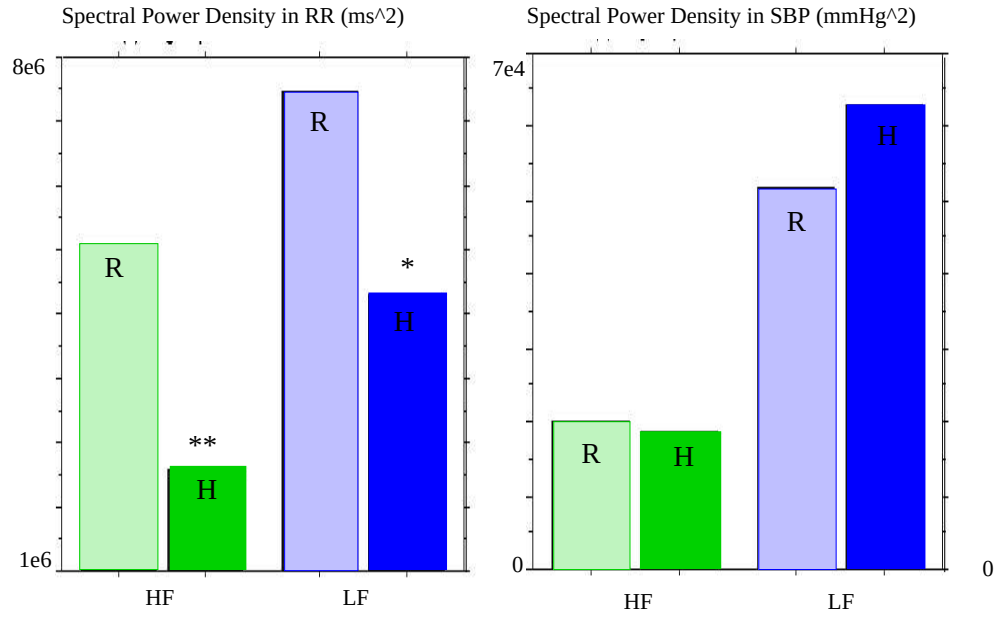

Figure 24: Mean values of the power spectra in HF (green) and LF (blue) bands. The left picture concerns RR (HF_{RR},LF_{RR}), the right picture concerns SBP (HF_{SBP},LF_{SBP}); R stands for Recovery and H for handgrip bouts.

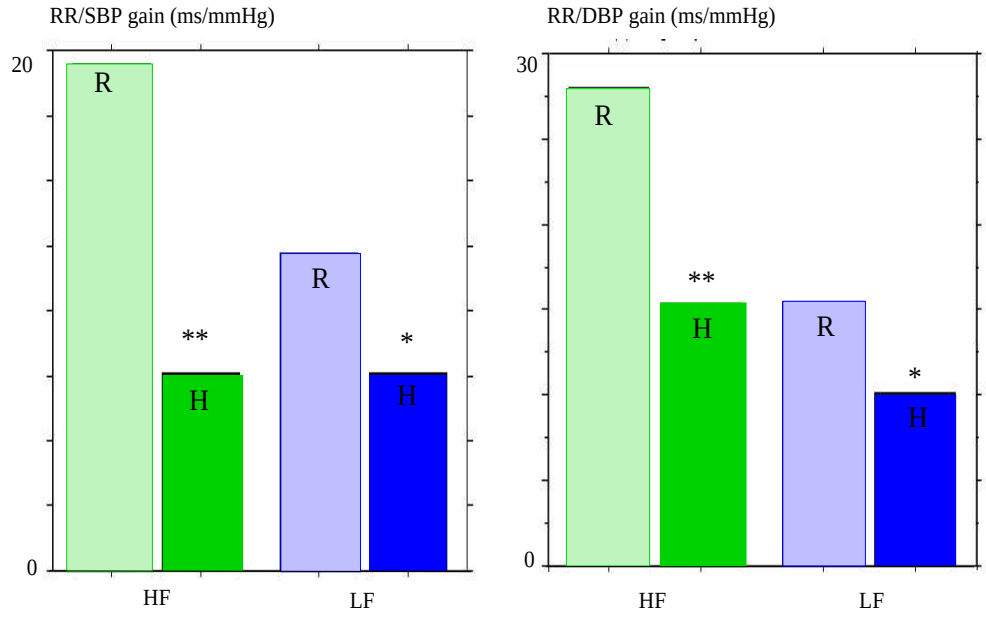

Figure 25: Mean values of the BRS in HF (green) and LF (blue) bands. The left picture represents gain between RR and SBP (gHF_{SBP} and gLF_{SBP}), the right picture represents the gain between RR and DBP (gHF_{DBP} and gLF_{DBP}); R stands for Recovery and H for handgrip bouts.

Values	Recovery	Handgrip	Wilcoxon p
Mean values			
RR	0.1025E+04 $\pm$ 0.81E+02	0.811E+03 $\pm$ 0.53E+02	** 0.01
SBP	0.148E+03 $\pm$ 0.6E+01	0.183E+03 $\pm$ 0.3E+01	** 0.01
DBP	0.80E+02 $\pm$ 0.3E+01	0.99E+02 $\pm$ 0.2E+01	** 0.01
Power spectral values			
HF_{RR}	0.5E+07 $\pm$ 0.2E+07	0.15E+07 $\pm$ 0.6E+06	** 0.01
LF_{RR}	0.75E+07 $\pm$ 0.25E+07	0.42E+07 $\pm$ 0.2E+07	* 0.02
HF_{SBP}	0.2E+05 $\pm$ 0.1E+05	0.19E+05 $\pm$ 0.4E+04	NS
LF_{SBP}	0.52E+05 $\pm$ 0.14E+05	0.63E+05 $\pm$ 0.25E+05	NS
HF_{DBP}	0.98E+04 $\pm$ 0.5E+04	0.48E+04 $\pm$ 0.2E+04	NS
LF_{DBP}	0.3E+05 $\pm$ 0.7E+04	0.25E+05 $\pm$ 0.65E+04	NS
Power normalized spectral values			
$HFnu_{RR}$	0.385E+0 $\pm$ 0.45E-01	0.306E+0 $\pm$ 0.67E-01	NS
$LFnu_{RR}$	0.615E+0 $\pm$ 0.45E-01	0.694E+0 $\pm$ 0.67E-01	NS
$HFnu_{SBP}$)	0.253E+0 $\pm$ 0.29E-01	0.309E+0 $\pm$ 0.62E-01	NS
$LFnu_{SBP}$	0.747E+0 $\pm$ 0.29E-01	0.691E+0 $\pm$ 0.62E-01	NS
$HFnu_{DBP}$	0.162E+0 $\pm$ 0.33E-01	0.181E+0 $\pm$ 0.4E-01	NS
$LFnu_{DBP}$	0.839E+0 $\pm$ 0.33E-01	0.819E+0 $\pm$ 0.4E-01	NS

Table 1: Mean values and power of spectral components of CV variables. Values are expressed as mean and Standard Error to Mean (SEM). RR unit is ms, $LF_{RR}, HF_{RR}, LFnu_{RR}, HFnu_{RR}$ units are ms^2/Hz. ABP unit is $mmHg$, $LF_{BP}, HF_{BP}, LFnu_{BP}, HFnu_{BP}$ units are $mmHg^2/Hz$. Significance: * 0.05>p>0.01; ** 0.01>p>0.001; NS p >=0.05. See Table of acronyms 6.

Mean values	RR	SBP
$CF_{Recovery}$	0.237E+0 $\pm$ 0.12E-01	0.228E+0 $\pm$ 0.67E-02
$CF_{Handgrip}$	0.223E+0 $\pm$ 0.22E-01	0.206E+0 $\pm$ 0.1E+0
$DI_{Recovery}$	0.105E+0 $\pm$ 0.15E-01	0.114E+0 $\pm$ 0.17E-01
$DI_{Handgrip}$	0.110E+0 $\pm$ 0.18E-01	0.088E+0 $\pm$ 0.17E-01

Table 2: Central Frequency (CF) and Dispersion Index (DI) for the HF spectrum in the RR and SBP time series. CF is expressed in Hz, DI is in (0;1). Values are expressed as mean and Standard Error to Mean (SEM). No significant difference appears between RR and SBP values neither between recovery and handgrip bout (Wilcoxon paired test).

Values	Recovery	Handgrip	Wilcoxon p
gHF_{SBP}	0.195E+02 $\pm$ 0.45E+01	0.76E+01 $\pm$ 0.176E+01	** 0.01
gLF_{SBP}	0.121E+02 $\pm$ 0.22E+01	0.76E+01 $\pm$ 0.166E+01	* 0.02
gHF_{DBP}	0.279E+02 $\pm$ 0.40E+01	0.153E+02 $\pm$ 0.342E+01	** 0.01
gLF_{DBP}	0.155E+02 $\pm$ 0.24E+01	0.101E+02 $\pm$ 0.215E+01	* 0.02

Table 3: Baroreflex sensitivity: gain between RR-interval and arterial blood pressure. Values are expressed as mean and Standard Error to Mean (SEM), in ms/mmHg. Significance: * 0.05>p>0.01; ** 0.01>p>0.001; NS p $>=$0.05. See Table of acronyms 6.

6 Discussion

6.1 On mean cardiovascular values

6.1.1 Positive staircase or treppe effect

Vagal cardiac withdrawal In this study, the treppe effect can be assessed because the first minute of the handgrip test stays for the must under only parasympathetic tone withdrawal without marked sympathetic effect. Our results comfort this knowledge:

The heart rate acceleration is the first change that one can notice, followed by marked ABP augmentation. Conversely, heart rate deceleration is followed by ABP decrease. The fastness of the RR response at the begining as well as at the end of the handgrip bout is characteristic of a vagal response. The acceleration begins at the onset of the handgrip bout and progressively increases throughout this phase, corresponding to vagal withdrawl. The deceleration suddenly occurs at the offset of the exercise, corresponding to vagal recovery(Fig.17, 18).

The mean RR time series of seven of the height subjects during handgrip bouts: $847 \pm 122ms$. This range of heart rate, lower than intrinsic rate, remains for the most in the range of vagal influence (Fig.26).

LF_{SBP} does not show significant difference between handgrip and recovery bouts. This absence of changes could be explained by the same level of the baroreflex control loop activity, thus by the absence of vascular sympathetic activation. This hypothesis is comforted by another study about voluntary apnea (not yet pubished). The end of apnea is marked by a peripheral vasoconstriction which leads to an ABP augmentation. An index of this vasoconstriction is extracted from the Pulse Arterial Tone (PAT) [Itamar Medical] [5]. We found that the increase in vasoconstriction is strongly related to an augmentation of the LF_{SBP} activity (Fig.27).

So, the fast inotropic (negative or positive) effect on the SBP (diminution or augmentation) depends only on the chronotropic (negative or positive) parasympathetic effect.

Delays between HR and SBP variations ABP and HR changes are very close as showed on figure 19. We have focused on the instant of cardiac deceleration because the changes are rapid enough to precisely measure delays between heart rate and SBP variations. The figure 20 shows the very fast response of the SBP to the sudden cardiac deceleration at the end of the exercise ($< 2s$). The treppe effect, i.e direct effect of heart rate on contractility is described in the physiological introduction. In a middle range of heart frequencies, a cardiac acceleration leads to an augmentation of the contractility, hence an augmentation of the ejection and ABP amplitude. On the contrary, a cardiac deceleration leads to a diminution of the ABP amplitude, as shown on figure 28.

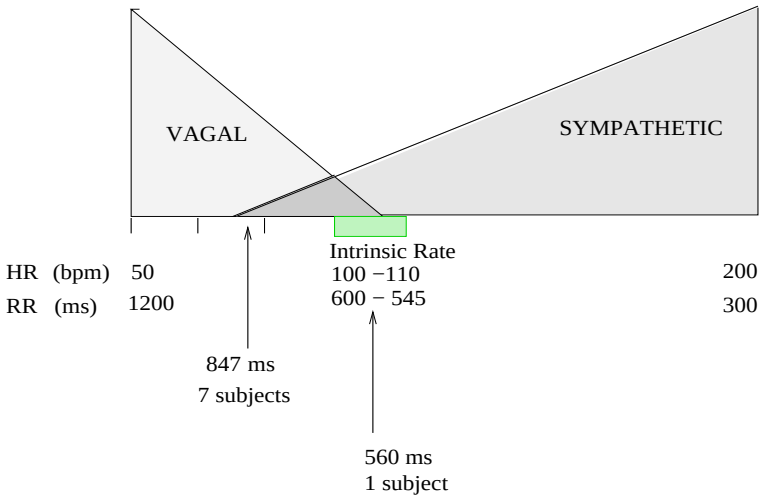

Figure 26: *Range of mean heart rate during handgrip bouts.*

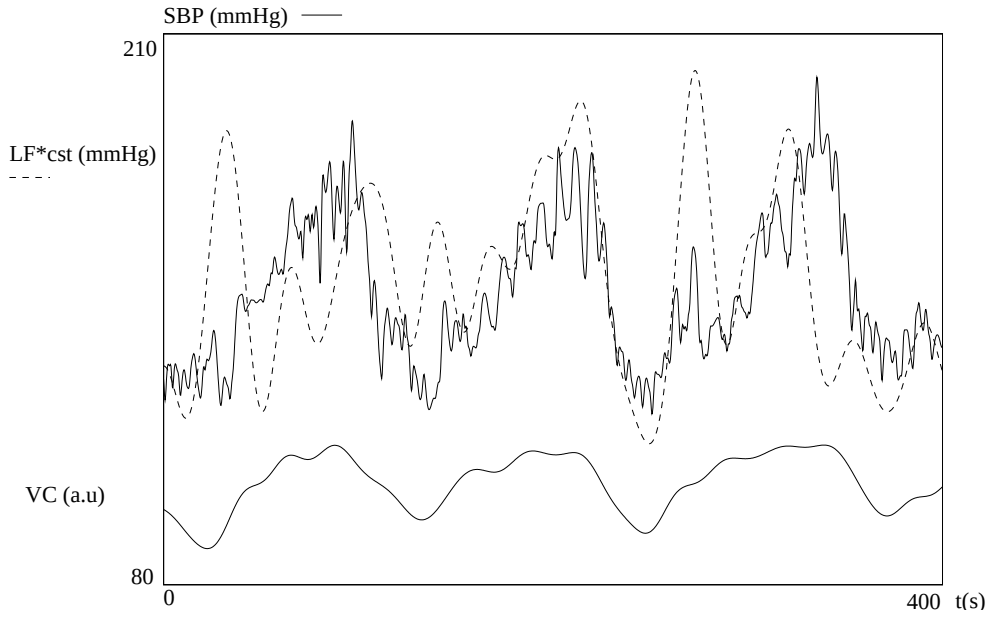

Figure 27: *Simultaneous time evolution of the parameters implied in sympathetic vacular activation during voluntary apnea in one subject: raw SBP, instantaneous LF-SBP and instantaneous index of peripheral vasoconstriction (VC).*

For all subjects (represented by A) except one (B), cardiac deceleration occurs a few seconds before SBP fall. For B, SBP fall occurs before cardiac deceleration and constantly when heart rate reachs 115 bpm. The B heart rate is a lot faster than the others: during the handgrip bout, the maximal heart rate for the seven subjects represented by A is 88 ± 12 bpm, thus the fastest heart rate does not exceed 100 bpm. For B, the smallest peak is greater than 115 bpm, the maximal is equal to 127 bpm. We could then hypothesise than 115 bpm is the frequency threshold of the treppe effect for the subject B [17], [21].

Strong linear correlation between HR and SBP For each subject, one bout of simultaneous increasing (decreasing) HR and SBP time series was selected. The mean R^2 simple regression coefficient was 0.937 ± 0.050 for increasing bouts (mean duration $58 \pm 10sec.$), and 0.954 ± 0.036 for decreasing bouts (mean duration $22 \pm 3sec.$), meaning that more than 90 % of SBP variability is explained by HR.

Evaluation of an index of the Stroke volume The mean blood pressure (MBP) is the product of the Stroke Volume (SV), the Heart Rate (HR) and the peripheral resistances (PR): $MBP = SV * HR * PR$ and $SV * PR = MBP/HR$. As PR could be lowered by cholinergic mechanisms [53], an increase of the SV-PR product emphasizes SV increase. The maxima of this SV-RP index for each handgrip bout of seven subjects have been averaged. The mean SV value is stable over the five handgrip bouts, there is no significance at the non parametric Friedman test (Table4 and Fig.29). The top of the figures 30, 31 shows the evolution of this SV index, over five handgrip bouts for 2 different subjects. The first subject exhibits a SV index increase, stabilised from the second handgrip bout. The second subject exhibits a more progressive SV index increase, stabilised at the fourth exercise.

6.1.2 Repetition effect on the Stroke Work

The Stroke Work (SW) represents the work done by the ventricle to eject blood into aorta. Sometimes, SW is simplified to $SW = SV * MAP$, using mean aortic pressure (MAP) instead of intraventricular pressure (in "Cardiovascular Physiology Concepts", Richard E. Klabunde, Ph.D.). Considering that MBP is close to MAP, we can assess the following SW index: $SW = SV * MBP$. The maxima of the SW index for each handgrip bout of seven subjects have been averaged. The mean SW value clearly increases over the four first handgrip bouts, significantly at the non parametric Friedman test (Table4 and Fig.29). The figures 30, 31 show the time representation of SW over five handgrip bouts followed by recovery bouts for two subjects. We can hypothesise that an increase in motor unit recruiting in the muscle at exertion occurs with the muscle fatigue. Thus, this progressive increasing muscle activation entails a parallel increase in HR and SBP [12].

	HG 1	HG 2	HG 3	HG 4	HG 5	Friedman p.
SV	1.83 ± 0.15	1.89 ± 0.15	1.92 ± 0.15	1.93 ± 0.15	1.91 ± 0.13	NS
SW	212 ± 20	230 ± 19	245 ± 21	258 ± 28	249 ± 24	** 0.02

Table 4: Mean and Standard Error to Mean (SEM) of the maximal values for the SV and SW indexes for each handgrip bout of seven subjects. Significance: * 0.05>p>0.01; NS p >=0.05.

The one-minute handgrip test is the alone physiological condition of cardiac acceleration for which the sympathetic is not involved, hence it is the alone condition to evidence treppe effect on CV signals. The treppe effect could explain how CV responses in heart rate and in systolic pressure are quasi simultaneous, to correctly adapt the CV system to sudden changes.

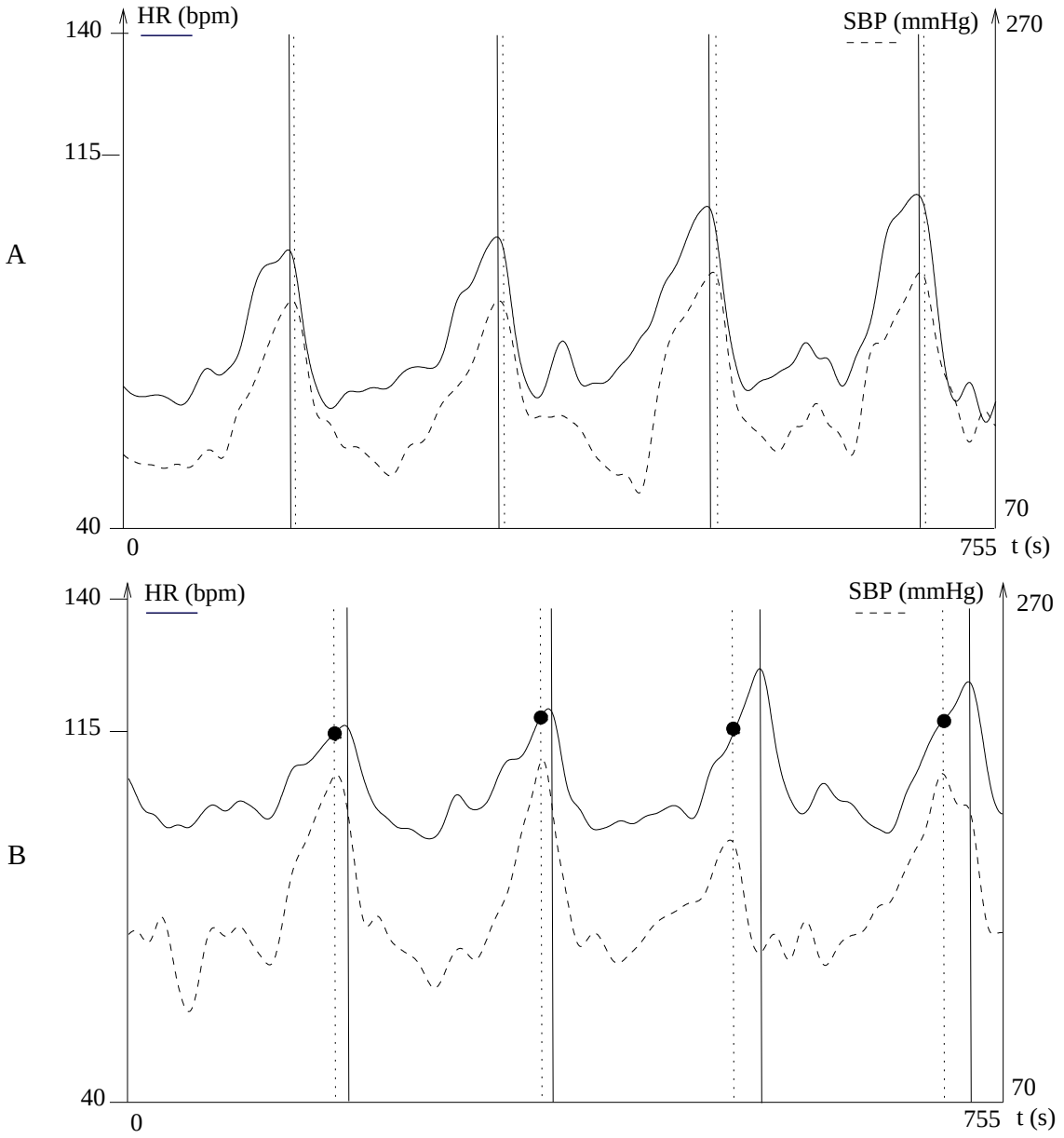

Figure 28: Heart rate and SBP time series over four successive handgrip bouts. A represents seven of the eight subjects: HR fall always precedes SBP fall, HR never reachs 115 bpm. B represents one subject: HR fall always follows SBP fall, SBP fall occurs when HR reachs 115 bpm.

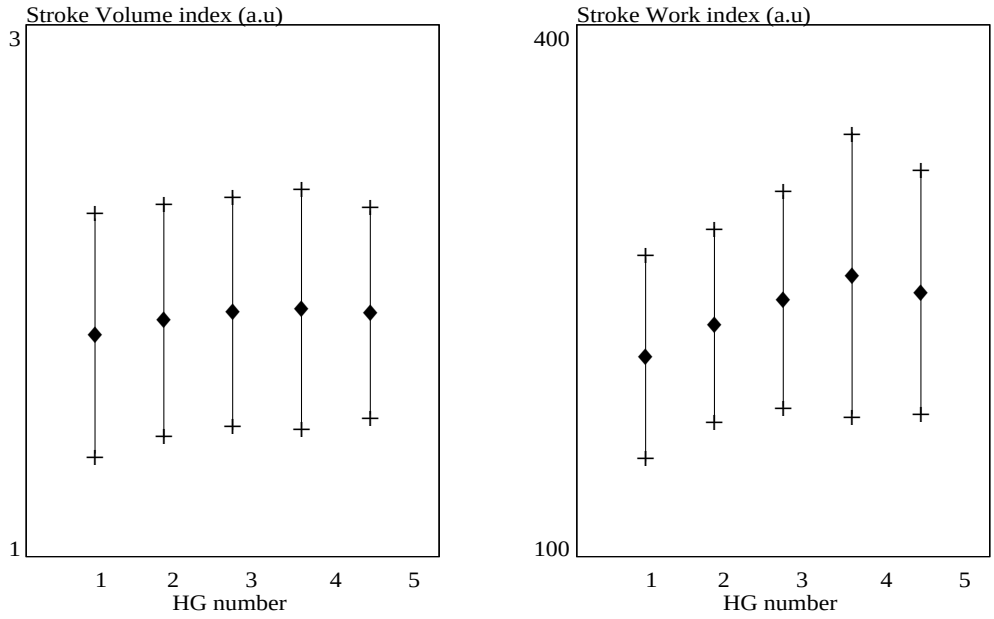

Figure 29: Mean and standard-deviation of the maximal values for the SVand SW indexes for each handgrip bout of seven subjects.

6.2 On spectral cardiovascular values and baroreflex sensitivity

6.2.1 On RR spectral values

In various studies, results exhibit an opposition between relatives values of the HF and LF spectral components ($HFnu_{RR}$, $LFnu_{RR}$), underlying the concept of an autonomic balance [36]. This "balance" can shift towards predominant vagal or sympathetic modulation, according to physiological conditions. The orthostatic head-up Tilt test exhibits a shift of the autonomic balance towards a sympathetic modulation from supine to standing [4], [20]. It is the same for Sleep from NREM to REM (Rapid Eye Movements) state [35]. Yet absolute values show an HF decrease for Tilt test and a LF increase for Sleep (see table 5. With the handgrip test, no change in the autonomic balance is found, whereas HF and LF spectral energies significantly fall together during the handgrip bout. These results strongly support the necessity of taking into account spectral absolute values in addition to normalised values, as still debated [36].

6.2.2 On RR and SBP spectral values and Baroreflex Sensitivity

It is surprising to consider that RR absolute spectral values exhibit together a sudden fall whereas ABP values remain stable from the recovery to the handgrip bout, as if the CV control was dissociated in modulating the oscillations around RR and ABP mean values.

In high frequency variability The influence of breathing on heart rate and on ABP is mainly mediated by autonomic central and mechanical peripheric mechanisms [55]. On the RR, the HF spectral power fall is mainly due to the vagal cardiac withdrawal, dependent on the central mechanism.
The absence of changes in ABP mediated by the mechanical mechanism, are compatible with an absence of

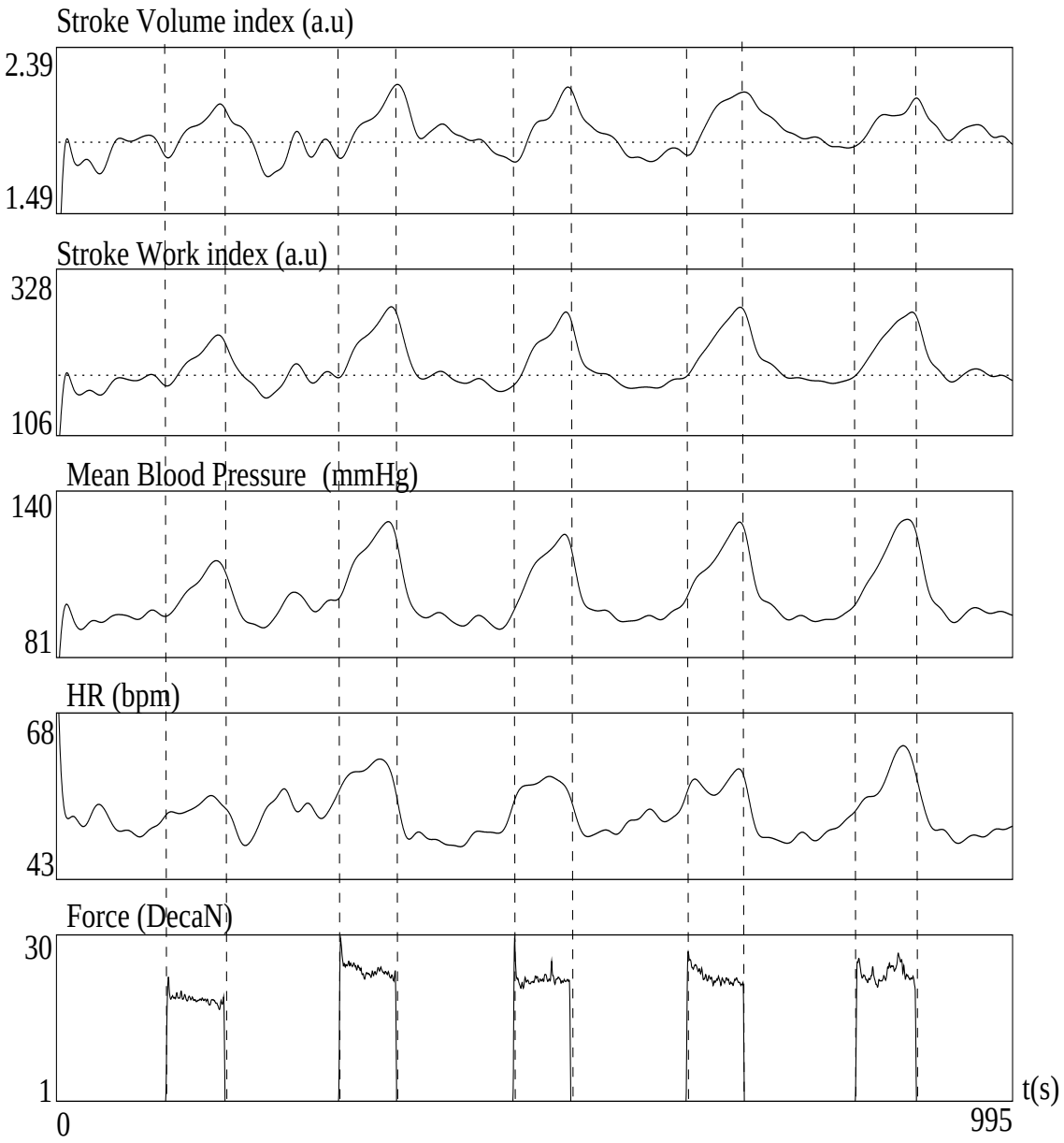

Figure 30: Time evolution of Stroke Volume (SV), Stroke Work (SW), Mean Blood Pressure (MBP) and Heart Rate (HR) over five handgrip bouts followed by recovery bouts in subject 1. These parameters are stabilised from the second handgrip bout.

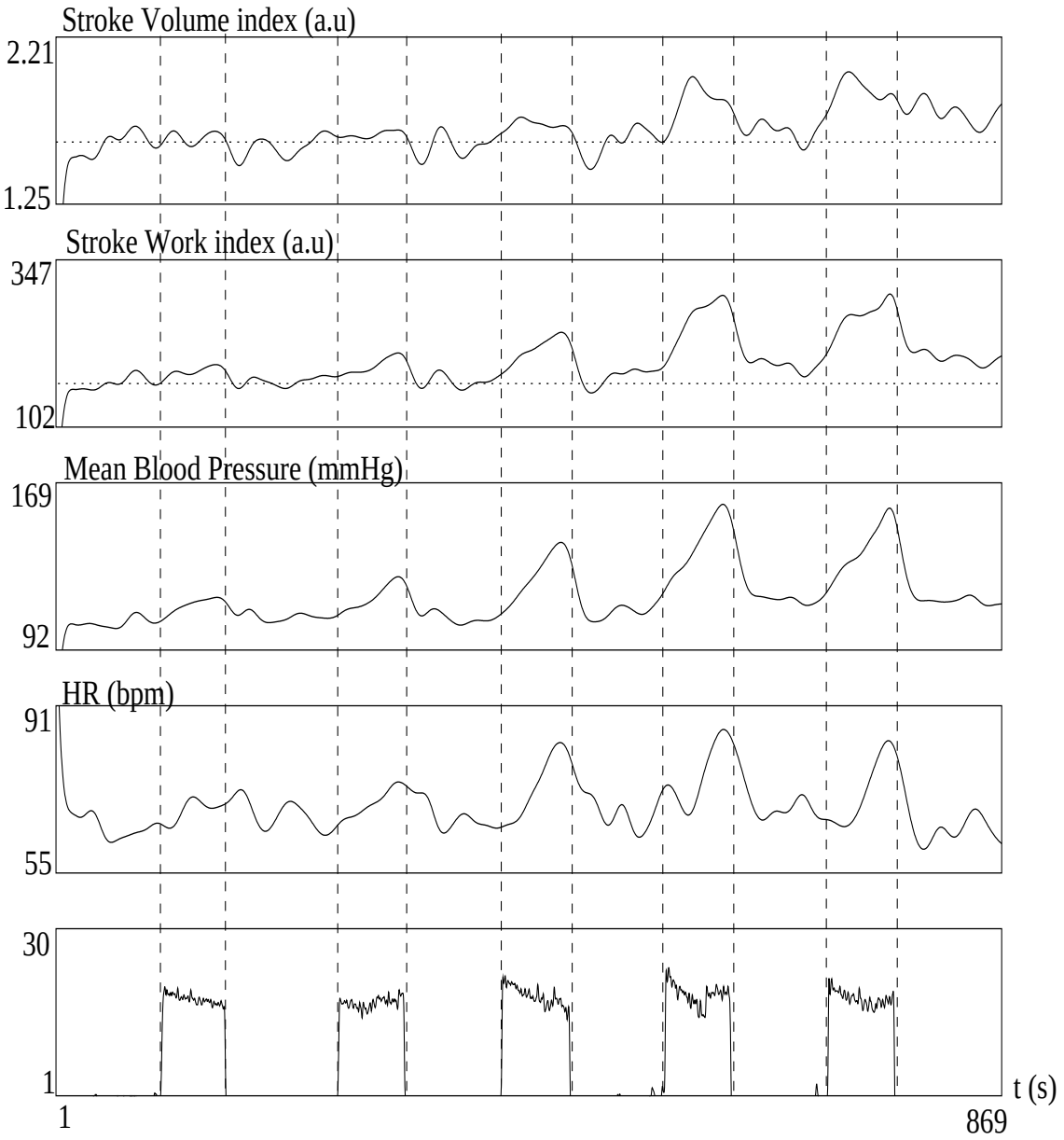

Figure 31: Time evolution of Stroke Volume (SV), Stroke Work (SW), Mean Blood Pressure (MBP) and Heart Rate (HR) over five handgrip bouts followed by recovery bouts in subject 2. These parameters progressively increase and are all stabilised from the fourth handgrip bout.

changes in breathing. Indeed, central frequency (CF), dispersion (DI) and power (HF_{SBP}, HF_{DBP}) of the HF spectrum remain constant between recovery and handgrip bouts (Tables 1 and 2.

In low frequency variability Two mechanisms have been proposed: a resonance due to the slow peripheral sympathetic control loop of vascular resistance in response to beat-to-beat changes in ABP [54], [59], [60], [63]) and a central rhythmic modulation of neural activity ([7], [32]). Morever, particular situations of open loop (pharmacological cardiac blockade, LVA etc) have shown that LF variablity in ABP and RR are not dependent [59]. In our point of view, these two mechanisms are working together in physiological conditions. The absence of changes in LF_{SBP} between recovery and handgrip bout could be explained by the same level of the baroreflex control loop activity, as sympathetic activation is not involved in the first minute of an handgrip test (see paragraph *staircase effect*). However, it is difficult to explain how LF_{RR} variability is so attenuated, unless we suppose an opening of the CV control loop.

Baroreflex Sensitivity The very significant diminution of the gains of the baroreflex loop in high and low frequencies directly depends upon the diminution of RR variabilities.

6.2.3 Cardiovascular control loop with two feedback levels

The figure 32 represents our model of the CV control at the atrial and ventricular levels. In our point of view, according to autonomic fibers distribution, atrium and ventricle are controlled in frequency and in amplitude. At atrial level, vagal afferences are concentrated on the sino-atrial node (SAN) and the atrio-ventricular node (AVN); sympathetic afferences are distributed on all myocardiac cells. At ventricular level, only sympathetic afferences are distributed (see section one). In this model, the vagal control, concentrated, acts on delays (described as dromotropic effect): D_{TP}, delay between the end of repolarisation (T wave) and the beginning of atrial depolarisation (P wave) and D_{AV}, atrio-ventricular delay. The sympathetic control has distributed inotropic ($I_{A+}, I_{A-}, I_{V+}, I_{V-}$), and bathmotropic effects (B_V, B_A). I_+ stands for inotropic effect on contractility during systole, I_- stands for inotropic effect on relaxation during diastole. PP interval is the result of chronotropic effects, dissociated in bathmotropic and dromotropic.
$PP = \rho_A B + D_{AV} + \rho_V B + D_{TP}$ where ρ_A and ρ_B stand for constants dependent upon atrium and ventricle.
PP can be decomposed into the intervals $PR = \rho_A B + D_{AV}$ and $RP = \rho_V B + D_{TP}$.

Our results agree with the hypothesis of two dissociated commands in frequency and in amplitude on the pacemaker node and myocardial tissue. This hypothesis allows to explain at the same time, the changes in the mean values of RR and ABP signals, the changes in their variabilities in HF and LF and the dependence of LF upon HF variability. In physiological conditions, the system acts as a closed loop with two feedback levels: a proportional instantaneous atrial feedback, driven first by vagal control; a proportional integral derivative (PID) ventricular feedback, driven by sympathetic control. In handgrip test, the massive vagal withdrawal opens the atrial loop which becomes a feedfoward drive. It allows a very fast response in frequency (RR diminution), and in amplitude (ABP augmentation) by the mean of the treppe effect. However, as the atrial loop is open, RR oscillations are attenuated. At the same time, the sympathetic feedback loop at the ventricular level is maintained on the ABP control, so the ABP oscillations remain stable. The diminution of the baroreflex gain between RR and ABP naturally results from the opening of the loop.
Thus, the expression of LF oscillations seems depending upon HF oscillations at atrial level in case of open loop: the mechanism could be a multiplier effect such as if vagal oscillations are inhibited or reduced then sympathetic oscillations cannot be entirely expressed.

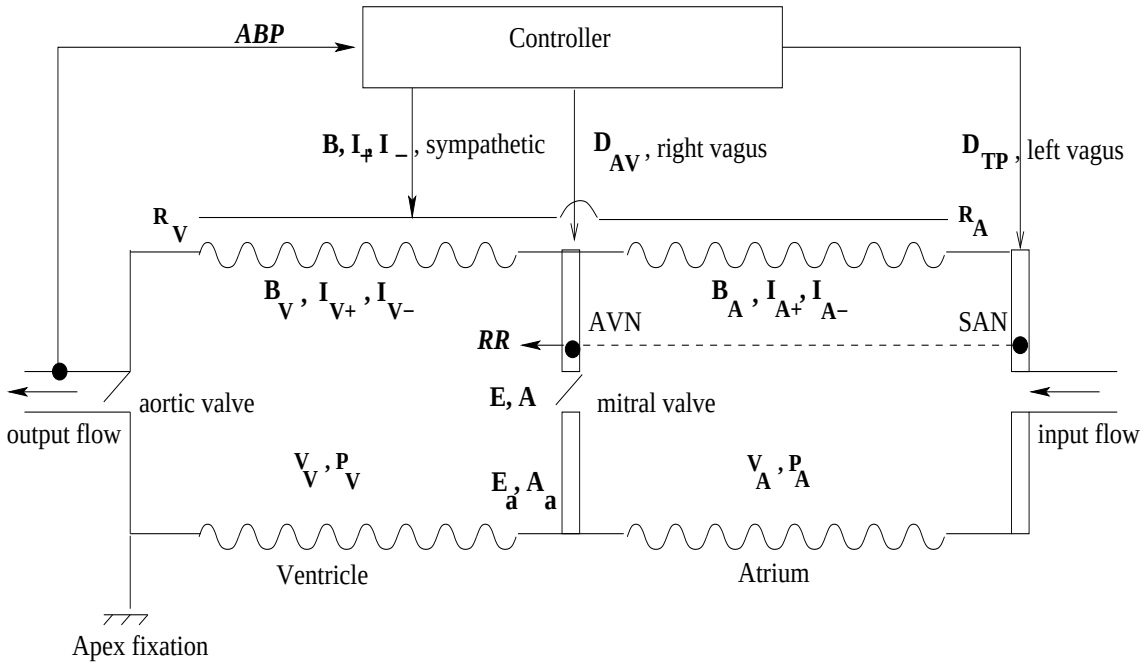

Autonomic effects

1) Chronotropic
B: Bathmotropic −on excitability, thus on propagation velocity
D: Dromotropic − on delay control of the sino−atrial node (SAN): D_{TP} (T and P waves)
− on delay control of the atrio−ventricular node (AVN) : D_{AV}
2) I: Inotropic − on intensity of contraction (I_+)/relaxation (I_-)
R_A , R_V : atrial and ventricular receptors;

Mechanical effects

E, A: Early and Atrial flows ; E_a, A_a:Early and Atrial annulus velocity
V_A , V_V : atrial and ventricular volumes
P_A, P_V: atrial and ventricular pressures

Figure 32: The CV autonomic control at the atrial and ventricular levels.

6.3 Towards a better understanding of other conditions

6.3.1 Heart rate variability at exercise

Handrgip is a condition of vagal withdrawal without sympathetic cardiac activation. The two following studies concern exercise but at two different heart rates; exercise is condition of parasympathetic withdrawal with sympathetic cardiac stimulation, despite peripheral vasodilatation; HRV has the same behavior as in the handgrip test: simultaneous disappearance of the HF and LF oscillations.

The first study was performed with 11 well trained pubertal subjects, on cycle ergometer below ventilatory threshold, corresponding to moderate exercise [8]. Figure 33 shows RR and HRV evolution from recovery to exercise: while RR decreases from 700 ms to 500 ms, HF and LF amplitudes progressively decrease together. RR is influenced first by vagal withdrawal followed by sympathetic activation (see Fig.6).

The second study was performed with height well trained adults on cycle ergometer above ventilatory threshold during a square-wave exercise [43]. In this case, heart rate is yet under autonomic influence (from 470 ms to 320 ms) but only under sympathetic cardiac activation (Fig.34). There is no more vagal influence under 500-600 ms and no more autonomic influence under 300 ms (Fig.6). RR and HRV progressively decrease together, as in the first study.

These studies support handgrip results and show that, even is the sympathetic is strongly activated, LF oscillations decrease with HF, due to the opening of the loop.

6.3.2 Baroreflex sensitivity during sleep and head-up tilt test

DBP values were discarded from the discussion as DBP involves vascular passive elements in addition to autonomic influences.

In Sleep Mean RR and ABP remain stable, as there is no particular need to change the level (such as an increase in oxygene uptake ...). There is only change in LF RR oscillations and thus in the baroreflex gain in low frequency (gLF_{SBP}), when shifting from NREM to REM sleep state (Table 5). During REM state the increase neural long term control could more effectively buffer CV perturbations secondary to bursts of brainstem stimulation during phasic epochs and could also maintain a strong CV control during longer tonic epochs [35]. The control loop is close, there is no vagal withdrawal and the sympathetic cardiac activation can be efficient. Thus, the increase in the LF gain evidences a working regulatory mechanism.

In head-up tilt test To prevent ABP from falling with the standing position, two mechanisms occur: a fast vagal cardiac withdrawal and a vascular sympathetic activation [4], [20]. Not surprising, RR mean and HF_{RR} values suddenly fall, exactly as in handgrip bout. LF_{SBP} is increased but LF_{RR} has no change (5). The enhancement of peripheral resistances provokes a normal activation of the baroreflex loop, explaining the LF_{SBP} increase. When bringing up the hypothesis of the atrial open loop, it becomes possible to understand the absence of change in the LF_{RR} oscillations. The atrial loop is open, the cardiac origin of sympathetic stimulation cannot be expressed, but, instead of its decrease as in the handgrip bout, the residual LF_{RR} could be due to the transmission of a part of the enhanced LF_{SBP}. As in the handgrip bout, the baroreflex gains are significantly decreased (Table 5).

Interpretation of a combination of four parameters: RR mean, HF_{RR}, gLF_{SBP}, gHF_{SBP} The three studies, handgrip test, Tilt test, Sleep states, exhibit various changes in mean and spectral values of RR and ABP,

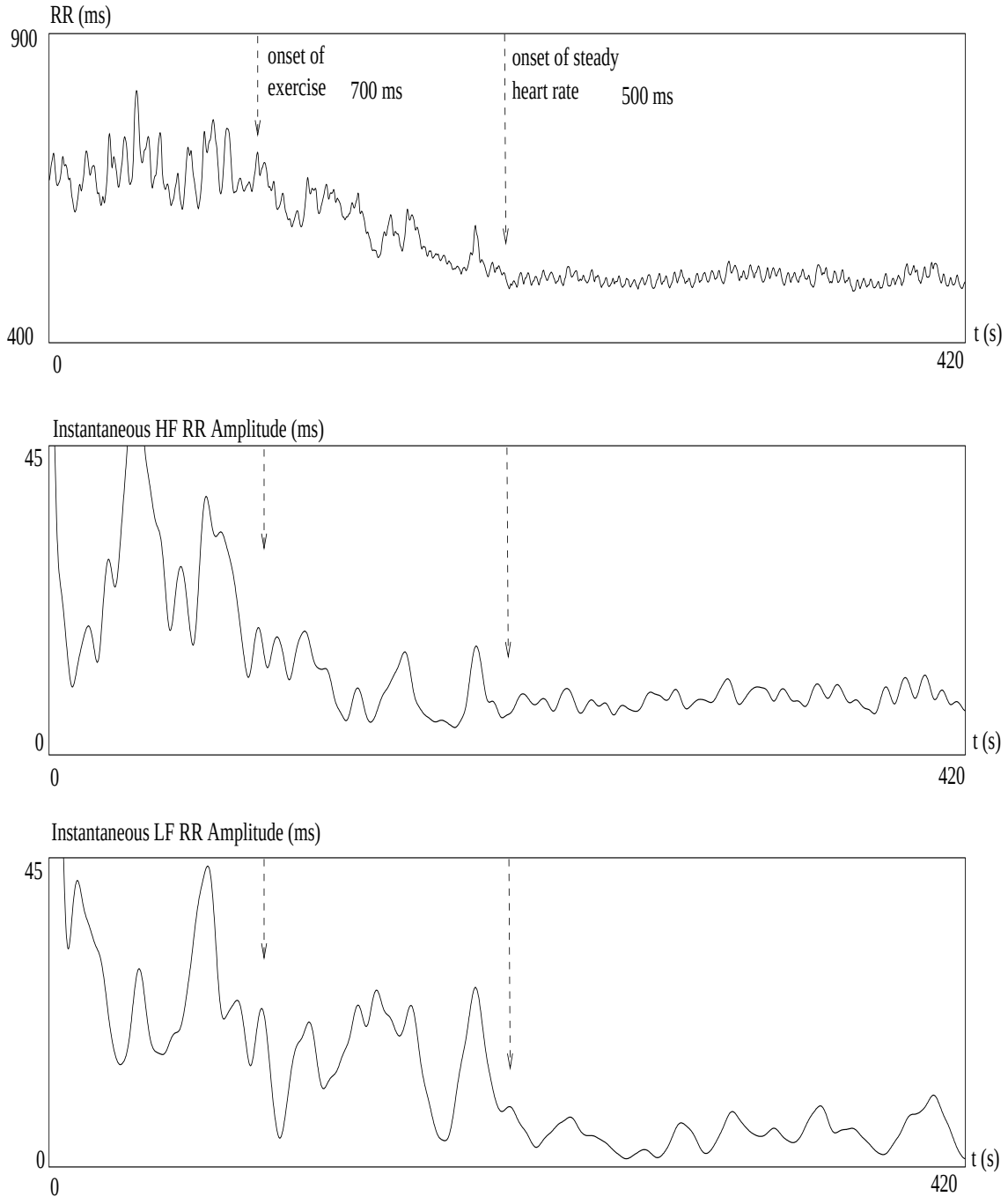

Figure 33: RR time series and RR variability of a representative pubertal subject during exercise below ventilatory threshold; RR values decreases from 850 to 500 ms, under vagal withdrawal followed by sympathetic activation.

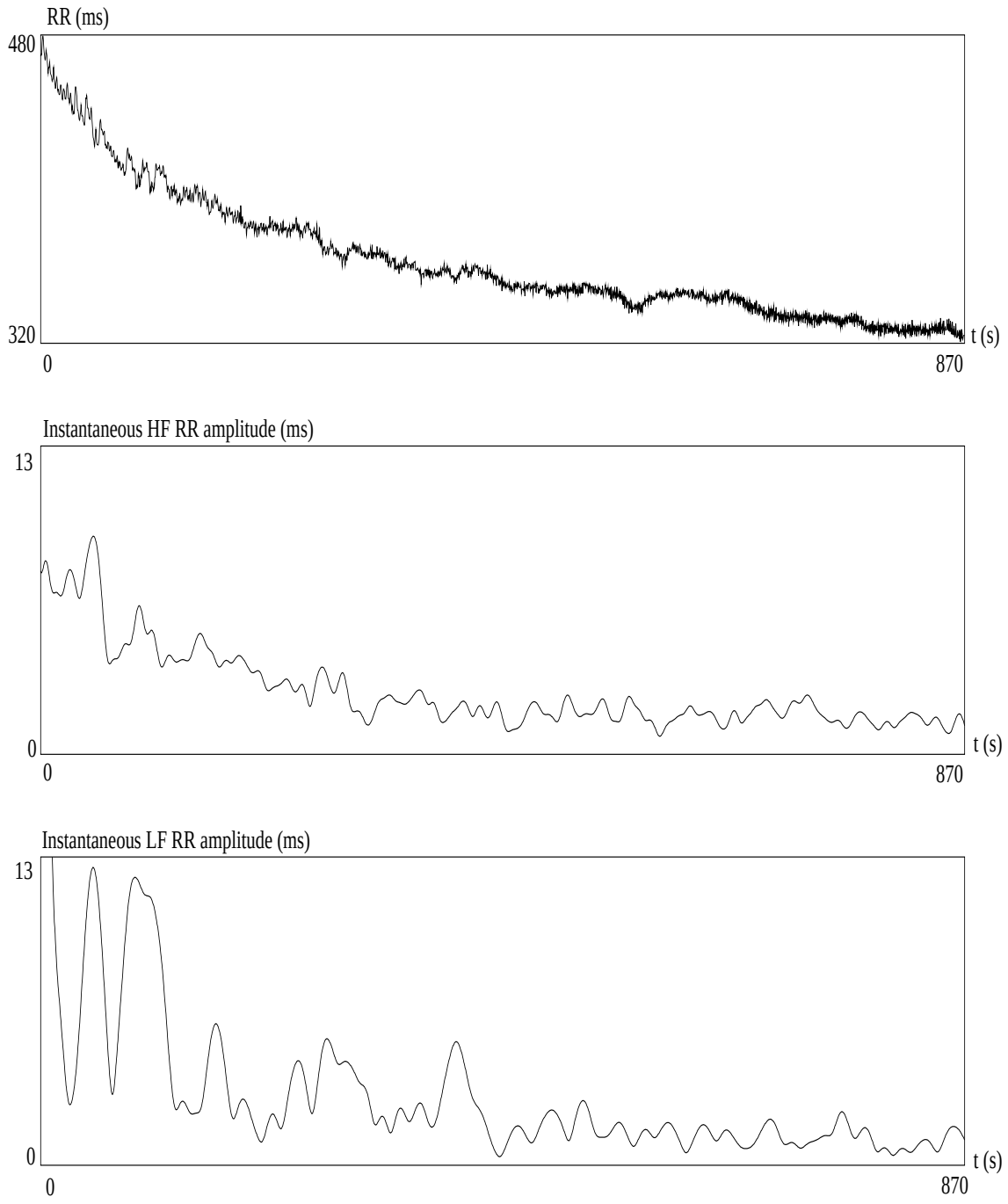

Figure 34: RR time series and RR variability of a representative adult subject during exercise above ventilatory threshold; RR values decreases from 480 to 320 ms, under sympathetic activation.

according to the underlying mechanisms (vagal/sympathetic cardiac activation/withdrawal, sympathetic vascular activation).

However, the simultaneous decrease of the four parameters, RR mean, HF_{RR} spectral power, LF and HF gains seems to provide an univocal information on the controller state. A simultaneous decrease in mean RR and HF_{RR} is the expression of a vagal withdraw (in stable ventilatory condition) as HF_{RR} is known to reflect only vagal drive. When this vagal withdraw is important enough to control a strong transition such as in handgrip and Tilt tests, the controller, by opening the atrial loop, decreases all RR oscillations and thus, necessary lowers the short and long term gains (gHF_{SBP}, gLF_{SBP}), whatever SBP oscillations are (Table5).

	Handgrip test	Tilt test	Sleep
	Recovery/Handgrip	Supine/Standing	NREM/REM
Subjects	8	9	12
Mean values			
RR	$\searrow$*	$\searrow$*	$\rightarrow$
SBP	$\nearrow$	$\rightarrow$	$\rightarrow$
RR power spectral values			
HF_{RR}	$\searrow$*	$\searrow$*	$\rightarrow$
LF_{RR}	$\searrow$	$\rightarrow$	$\nearrow$
$HFnu_{RR}$	$\rightarrow$	$\searrow$	$\searrow$
$LFnu_{RR}$	$\rightarrow$	$\nearrow$	$\nearrow$
SBP power spectral values			
HF_{SBP}	$\rightarrow$	$\nearrow$	$\rightarrow$
LF_{SBP}	$\rightarrow$	$\nearrow$	$\rightarrow$
Baroreflex Sensitivity			
gHF_{SBP}	$\searrow$*	$\searrow$*	$\nearrow$
gLF_{SBP}	$\searrow$*	$\searrow$*	$\nearrow$

Table 5: RR and ABP mean values, RR and SBP spectral values comparisons between three studies involving ANS changes. The stars point out the four parameters together evocative of an atrial feedforward.

7 Conclusion

The handgrip isometric test only involves vagal response during the first minute. This particular physiological condition allows us to better understand the CV autonomic control mechanisms implied at the beginning of an exercise. To anticipate an increase in oxygen needs, the controller elicits an increase in cardiac rate (shortening of the RR interval) and contractility (SBP increase). Even if oxygen needs remain stable in the handgrip test, the controller acts 'as if', that is deleterious for the organism but represents a good model for any kind of exercise, isometric or isotonic. To respond in emergency, the fastest control, mediated by the vagus nerve, is the first involved, consisting in a marked withdrawal, to assume the relay with the sympathetic control. This study gives evidence of two major mechanisms, together involved at the beginning of the handgrip test. The first is the positive staircase or treppe effect and is revealed by the analysis of RR and SBP raw time series. The second is the functionning of the controller at two feedback levels, atrial and ventricular, and is revealed by the changes in RR and SBP variability.

Treppe effect The only direct vagal effect is chronotropic, that could be insufficient to assume an actual increase in oxygen needs. The treppe effect that correlates contractility to heart rate then takes place to efficiently substitute the sympathetic inotropic effects. So, at the beginning of an exercise, a vagal withdrawal has effects close to a sympathetic activation on the heart. The treppe effect is revealed in the two cases of vagal changes: at the beginning of the handgrip bout, the chronotropic positive effect of the vagal withdrawal elicits an inotropic positive effect; at the end of the handgrip bout, the chronotropic negative effect of the vagal activation elicits a negative inotropic effect.

Two feedback levels of control The dissociation between RR and SBP variability during the handgrip test reveals the existence of two dissociated commands, in frequency at the atrial level and in amplitude at the ventricular level. At the atrial level, the controller acts like a feedforward to exert a fast response in frequency and so decreases RR variability; at the ventricular level, the controller maintains the sympathetic feedback in amplitude and thus the SBP variability remains stable. It is worth noticing that the stability of the amplitude of the SBP oscillations agrees with the absence of peripheral resistances activation during the first minute of the handgrip test.

Until now, only two measures for studying the baroreflex loop are avaivable, RR and ABP signals, which allow us to take into account the inotropic effect and a global chronotropic effect. The R peak represents the ventricular and not the atrial depolarisation, but it is often the alone event easily detectable from a single ECG derivation. The access to other ECG events is necessary to precisely detail the dromotropic and bathmotropic effects and the TP delay. In this way, the dynamic vectocardiography could be useful, simplifying P and T waves detection.

Acronym	Acronym meaning
CV	CardioVascular
HR	Heart Rate
HRV	Heart Rate Variability
ABP	Arterial Blood Pressure
SBP, DBP	Systolic, Diastolic Blood Pressure
MBP	Mean Blood Pressure
SV	Stroke Volume
SW	Stroke Work
BF	Breathing Frequency
ANS	Autonomic Nervous System
BRS	Baroreflex Sensitivity
HF_X, LF_X	High, Low Frequency spectral power of X (RR, ABP)
$HFnu_X, LFnu_X$	High, Low Frequency spectral power in normalised units
CF_X	Central frequency of the X (RR, SBP) spectrum in HF
DI_X	Dispersion Index of the X (RR, SBP) spectrum in HF
gHF_{ABP}, gLF_{ABP}	High, Low Frequency gain between SBP and DBP and RR
gHF_{SBP}, gLF_{SBP}	High, Low Frequency gain between SBP and RR
gHF_{DBP}, gLF_{DBP}	High, Low Frequency gain between DBP and RR

Table 6: Table of acronyms

References

[1] NR. Alpert, BJ Leavitt, FP. Ittleman, G. Hasenfus, B. Piseke, and LA. Mulieri. A mechanistic analysis of the force-frequency relation in non-failing and progressively failing human myocardium. *Basic Res Cardiology*, 93: Suppl.1:23–32, 1998.

[2] William H. Barry. $na^+ - ca^2+$ exchange in failing myocardium, friend or foe? *Circ Res.*, 87:529–531, 2000.

[3] SL. Beau, DE. Hand, RB. Schuessker, BI. Bromberg, B. Kwon, JP. Boineau, and JE. Saffitz. Relative densities of muscarinic cholinergic snd β-adrenergic receptors in the canine sinoatrial node and their relation to sites of pacemaker activity. *Circulation Research*, 77:957, 1995.

[4] J. Bestel, L. Mangin, C. Médigue, A. Monti, and M. Sorine. Proposition of an index of the autonomic nervous system activity in the arterial blood pressure short term regulation. Nancy, June 1998. Blood Pressure Variablity in Health and Disease, Satellite Symposium of the XVII^{e} Scientific Meeting of the International Society of Hypertension. Vol. 12, Suppl. 1 of the em Fundamental & Clinical Pharmacology journal.

[5] S. Bise. Le blocage respiratoire comme modèle de stress oxydatif lié au syndrome d'apnées du sommeil: adaptations cardiovasculaires et modifications des biomarqueurs du stress oxydatif dans les gaz exhalés. Rapport de d.e.a. physiologie et biomécanique de l'homme en mouvement. directeur: Dr yves papelier, Laboratoire: Biologie et Adaptations Cardio-Respiratoires et du Sommeil (Pr. Pierre Escourrou, Hôpital Antoine Béclère, 92141, Clamart, 2002-2003.

[6] Sun C. Choi. In *Introductory Applied Statistics in Science.*, pages 143–150. 1978.

[7] R.L. Cooley, N. Montano, C. Cogliati, P. Van De Borne, W. Richenbacher, R. Oren, and V.K. Somers. Evidence for a central origin of the low-frequency oscillation in rr-interval variability. *Circulation*, 98:556–561, 1998.

[8] F. Cottin, C. Médigue, PM. Leprêtre, Y. Papelier, JP. Koralsztein, and V. Billat. Heart rate variability during exercise performed above ventilatory threshold. *Medicine & Science in Sports & exercise*, 93: Suppl.1:594–600, 2004.

[9] Ph. Van de Borne, H. Nguyen, P. Biston, P. Linlowski, and J.P. Degaute. Effects of wake and sleep stages on the 24-h autonomic control of blood pressure and heart rate in recumbent men. *Am. J. Physiol.*, 266:H548–H554, 1994.

[10] D.L. Eckberg. Sympathovagal balance a critical appraisal. *Circulation*, 96:3224–3232, 1997.

[11] Task force of the European Society of Cardiology, the North American Society of pacing, and electrophysiology. Heart rate variability: standards of measurement, physiological interpretation, and clinical use. *Circulation*, 93:1043–1065, 1996.

[12] U. Freyschuss. Cardiovascular adjustment to somatomotor activation.the elicitation of increments in heart rate, aortic pressure and venomotor tone with the initiation of muscle contraction. *Acta Physiol Scand Suppl*, 342: 01-63, 1970.

[13] J.J. Goldberger, Y.H. Kim, M.W. Ahmed, and A.H. Kadish. Effect of graded increases in parasympathetic tone on heart rate variability. *J Cardiovasc Electrophysiol.*, 7 (7):594–602, 1996.

[14] J. Hansen, Thomas GD., Harris SA., Parsons WJ., and Victor RG. Differential sympathetic neural control of oxygenation in resting and exercising human skeletal muscle. *J Clin Invest.*, 98(2):584–96, 1996.

[15] SF. Hobbs. Central command during exercise: parallel activation of the cardiovascular and motor systems by descending command signals. In *Circulation, Neurobiology, and Behavior*, pages 217–232. 1982.

[16] SF. Hobbs and Gandevia SC. Cardiovascular responses and the sense of effort during attempts to contract paralysed muscles: role of the spinal cord. *Neurosci Lett 4*, 57(1):85–90, 1985.

[17] BD. Hoit, N. Ball, and RA. Walsh. Invasive hemodynamics and force-frequency relationships in open-versus closed-chest mice. *Special communication at the American Physiological Society*, pages H2528–H2532, 1997.

[18] H.B. Hopf, A. Skyschally, G. Heusch, and J. Peters. Low-frequency spectral power of heart rate variability is not a specific marker of cardiac sympathetic modulation. *Anesthesiology*, 82(3):609–619, 1995.

[19] R.L. Hughson, L. Quintin, G. Annat, Y. Yamamoto, and C. Gharib. Spontaneous baroreflex by sequence and power spectral methods in humans. *Clinical physiology*, 13:663–676, 1993.

[20] S. Jasson, C. Médigue, P. Maison-Blanche, N. Montano, L. Meyer, C. Vermeiren, P. Mansier, P. Coumel, A. Malliani, and B. Swynghedauw. Instant power spectrum analysis of heart rate variability during orthostatic tilt using a time-frequency domain method. *Circulation*, 96:3521–3526, 1997.

[21] VJ. Kadambi, N. Ball, EG. Kranias, RA. Walsh, and BD. Hoit. Modulation of force-frequency relation by phospholamban in genetically engineered mice. *Special communication at the American Physiological Society*, pages H2245–H2249, 1999.

[22] CA. Karle, E. Zitron, W. Zhang., S. Kathöfer, W. Schoels, and J. Kiehn. Rapid component $i_k r$ of the guinea-pig cardiac delayed rectifier k^+ current is inhibited by β_1-adrenoreceptor activation, via camp/protein kinase a_dependent pathways. *Cardiovascular Research*, 53:355–362, 2002.

[23] HA. Kluess, RH. Wood, and MA. Welsch. Vagal modulation of the heart and central hemodynamics during handgrip exercise. *Am J Physiol Heart Circ Physiol.*, 278(5):H1648–52, 2000.

[24] A. Kurita, B. Takase, H. Hikita, A. Uehata, T. Nishioka, H. Nagayoshi, K. Satomura, and S. Nakao. Frequency domain heart rate variability and plasma norepinephrine level in the coronary sinus during handgrip exercise. *Clin Cardiol*, 22:207–212, 1999.

[25] K. LoffelholzD and R. Lindmar. Acetylcholine synthesis and release in the heart. In *Vagal Control of the Heart: Experimental Basis and Clinical Implications*, chapter 10, pages 147–159. 1994.

[26] A. Malliani, M. Pagani, F. Lombardi, and S. Cerutti. Cardiovascular neural regulation explored in the frequency domain. *Circulation*, 84:482–492, 1991.

[27] A. Malliani, M. Pagani, N. Montano, and G. S. Mela. Sympathovagal balance: a reappraisal. *Circulation*, 98:2640–2643, 1998.

[28] L. Mangin, A. Monti, C. Médigue, I. Macquin-Mavier, M.E. Lopez, P. Gueret, A. Castaigne, J. Bestel, C. Baillard, B. Swynghedauw, and P. Mansier. Altered baroreflex gain during voluntary breathing in chronic heart failure. *European Journal of Heart Failure*, 3(2):189–195, 2001.

[29] DI. McCloskey. Centrally-generated commands and cardiovascular control in man. *Clin Exp Hypertens*, 3(3):369–378, 1981.

[30] C. Médigue, A. Girard, D. Laude, A. Monti, M. Wargon, and J.L. Elghozi. Relation between pulse interval and respiratory sinus arrhythmia: a time- and frequency-domain analysis of the effects of atropine. *Pflügers Archiv European Journal of Physiology*, (441):650–655, 2001.

[31] J. H. Mitchell and R. F. Schmidt. Cardiovascular reflex control by afferent fibers from skeletal muscle receptors. In *Handbook of Physiology. The Cardiovascular System. Peripheral Circulation and Organ Blood Flow*, volume III pt. 2, chapter 17, pages 623–658. 1983.

[32] N. Montano, T. Gnecchi-Ruscone, A. Porta, F. Lombardi, A. Malliani, and S.M. Barman. Presence of vasomotor and respiratory rhythms in the discharge of single medullary neurons involved in the regulation of cardiovascular system. *J Auton Nerv Syst.*, 57:116–122, 1996.

[33] A. Monti. *Modélisation et analyse des rythmes dans les systèmes respiratoire et cardiovasculaire.* Doctorat en sciences, Université de Paris XI, UFR scientifique d'Orsay, 2002.

[34] A. Monti, C. Médigue, and L. Mangin. Instantaneous parameter estimation in cardiovascular series by harmonic and time-frequency analysis. *IEEE Transactions on Biomedical Engineering*, 49 (12-2):1547–1556, 2002.

[35] A. Monti, C. Médigue, H. Nedelcoux, and P. Escourrou. Cardiovascular autonomic control during sleep in normal subjects. *European Journal of Applied Physiology*, 87:174–181, 2002.

[36] A. Monti, C. Médigue, and M. Sorine. Short-term control of the cardiovascular system: modelling and signal analysis. Rapport de recherche 4427, INRIA, Rocquencourt, 2002.

[37] C. Médigue, A. Monti, and A. Wambergue. Lary_cr: Software package for the analysis of cardio vascular and respiratory rhythms in the scicos-scilab environnment. Rapport technique 0259, INRIA, Rocquencourt, 2002.

[38] M. Nowak, Olsen KS., Law I., Holm S., Paulson OB., and Secher NH. Command-related distribution of regional cerebral blood flow during attempted handgrip. *J Appl Physiol.*, 86(3):819–24, 1999.

[39] M. Pagani. Spectral analysis of heart rate variability in the assessment of autonomic diabetic neuropathy. *J. Autonom. Nerv. Syst.*, 23:143–153, 1988.

[40] M. Pagani, F. Lombardi, and S. Guzzetti. Power spectral analysis of heart rate and arterial pressure variabilities as a marker of sympathovagal interaction in man and conscious dog. *Circ. Res.*, 59:178–193, 1986.

[41] J. Pan and WJ. Thompkins. A real time qrs detection algorithm. *IEEE Trans Biomed Eng*, 3:230–236, 1985.

[42] R.B. Panerai, M.A. James, J.F. Potter, L. Fan, and D.H. Evans. Baroreceptor sensitivity in human subjects: sequence or spectral analysis? *Computers in Cardiology*, pages 305–308, 1995.

[43] Y. Papelier, F. Clément, C. Médigue, F. Cottin, S. Bise, and P. Escourrou. Comparison of hr and vo2 kinetics during square wave exercise in human, 2003. soumis.

[44] Y. Papelier, P Escourrou., JP Gauthier., and LB Rowell. Carotid baroreflex control of blood pressure and heart rate in man during dynamic exercise. *J Appl Physiol*, 77(2):502–506, 1994.

[45] G. Parati, J.P. Saul, M. Di Rienzo, and G. Mancia. Spectral analysis of blood pressure and heart rate variability in evaluating cardiovascular regulation. *Hypertension*, 25:1276–1286, 1995.

[46] J. Parlow, J.P. Viale, G. Annat, R. Hughson, and L. Quintin. Spontaneous cardiac baroreflex in humans. comparison with drug-induced responses. *Hypertension*, 25:1058–1068, 1995.

[47] M. Piepoli, Clark AL., Volterrani M., Adamopoulos S., Sleight P., and Coats AJ. Contribution of muscle afferents to the hemodynamic, autonomic, and ventilatory responses to exercise in patients with chronic heart failure: effects of physical training. *Circulation.*, 93(5):940–52, 1996.

[48] M.V. Pitzalis, F. Mastropasqua, and F. Massari et al. Effect of respiratory rate on the relationships between rr interval and systolic blood pressure fluctuations: a frequency-dependent phenomenon. cardiovasc. *Research*, 38:332–339, 1998.

[49] JT. Potts, Shi XR., and Raven PB. Carotid baroreflex responsiveness during dynamic exercise in humans. *Am J Physiol*, 265(6 Pt 2):H1928–38, 1993.

[50] H.W. Robbe, L.J. Mulder, H. Ruddel, W.A. Langewitz, J.B. Veldman, and G. Mulder. Assessment of baroreceptor reflex sensitivity by means of spectral analysis. *Hypertension*, 10:538–543, 1987.

[51] LB. Rowell and O'Leary DS. Reflex control of the circulation during exercise: chemoreflexes and mechanoreflexes. *J Appl Physiol*, 69:407–418, 1990.

[52] M. Saito, H. Abe, S. Iwase, K. Koga, and T. Mano. Muscle sympathetic nerve responsiveness to static contraction is not altered under hypoxia. *Jpn J Physiol.*, 41(5):775–83, 1991.

[53] JS. Sanders, Mark AL., and Ferguson DW. Evidence for cholinergically mediated vasodilation at the beginning of isometric exercise in humans. *Circulation.*, 79(4):815–24, 1989.

[54] J.P. Saul, R.D. Berger, P. Albrecht, S.P. Stein, M.H. Chen, and R.J. Cohen. Transfer function analysis of the circulation: unique insights into cardiovascular regulation. *Am. J. Physiol.*, 261:H1231–H1245, 1991.

[55] J.P. Saul and Cohen R.J. Respiratory sinus arrhythmia. In NY Futura Publishing Co. Inc., Armonk, editor, *Vagal control of heart: experimental basis and clinical implications*, pages 511–536. Levy M.N and Swartz P.J., 1994.

[56] DR. Seals. Influence of muscle mass on sympathetic neural activation during isometric exercise. *J Appl Physiol.*, 67(5):1801–6, 1989.

[57] DR. Seals, Johnson DG., and Fregosi RF. Hypoxia potentiates exercise-induced sympathetic neural activation in humans. *J Appl Physiol*, 71(3):1032–1040, 1991.

[58] DR. Seals and Enoka RM. Sympathetic activation is associated with increases in emg during fatiguing exercise. *J Appl Physiol.*, 66(1):88–95, 1989.

[59] J.A. Taylor and D.L. Eckberg. Fundamental relations between short-term rr-interval and arterial pressure oscillations in humans. *Circulation*, 93:1527–1532, 1996.

[60] B.J. TenVoorde. *Modeling the baroreflex: a systems analysis approach*. PhD thesis, Vrije Universiteit, Enschede, 1992.

[61] PJ. Ferreira Tucci, N. Murad, CL. Rossi, RJ. Nogueira, and O. Santana. Heart rate modulates the slow enhancement of contraction due to sudden left ventricular dilatation. *Am J Physiol Heart Circ Physiol*, 280:H2136–2143, 2001.

[62] P. Valensi, Bich Ngoc PT., Idriss S., Paries J., Cazes P., Lormeau B., and Attali JR. Haemodynamic response to an isometric exercise test in obese patients: influence of autonomic dysfunction. *Int J Obes Relat Metab Disord.*, 23(5):543–9, 1999.

[63] C. Vermeiren. *Analyse et modélisation du système cardiovasculaire et sa régulation à court terme par le système nerveaux autonome*. Génie biologique et médical, Université de Paris Val de Marne, U.F.R. de Sciences et de Technologie, 1996.

[64] R. Vetter, JM. Vesin, P. Celka, and U.Scherrer. Observer of the human cardiac sympathetic nerve activity using noncausal blind source separation. *IEEE Trans Biomed Eng.*, 46(3):322–30, 1999.

[65] SF. Vissing, Scherrer U., and Victor RG. Stimulation of skin sympathetic nerve discharge by central command. differential control of sympathetic outflow to skin and skeletal muscle during static exercise. *Circ Res.*, 69(1):228–38, 1991.

[66] J.W. Williamson, R. McColl, and D. Mathews. Evidence for central command activation of the human cortex during exercise. *J Appl Physiol*, 94:1726–1734, 2003.

Unité de recherche INRIA Rocquencourt
Domaine de Voluceau - Rocquencourt - BP 105 - 78153 Le Chesnay Cedex (France)

Unité de recherche INRIA Lorraine : LORIA, Technopôle de Nancy-Brabois - Campus scientifi que
615, rue du Jardin Botanique - BP 101 - 54602 Villers-lès-Nancy Cedex (France)
Unité de recherche INRIA Rennes : IRISA, Campus universitaire de Beaulieu - 35042 Rennes Cedex (France)
Unité de recherche INRIA Rhône-Alpes : 655, avenue de l'Europe - 38330 Montbonnot-St-Martin (France)
Unité de recherche INRIA Sophia Antipolis : 2004, route des Lucioles - BP 93 - 06902 Sophia Antipolis Cedex (France)

Éditeur
INRIA - Domaine de Voluceau - Rocquencourt, BP 105 - 78153 Le Chesnay Cedex (France)
http://www.inria.fr
ISSN 0249-6399